TAMPERE UNIVERSITY OF TECHNOLOGY

FANNI MYLLÄRI

GAS–PARTICLE EQUILIBRIUM OF ALKALI METAL COMPOUNDS STUDIED IN AN AEROSOL TEST REACTOR

Master of Science thesis

Examiners: Professor Jorma Keskinen
Docent Topi Rönkkö
Examiners and topic approved in the Faculty Council of the Faculty of Natural Sciences
on the 6.2.2013

ABSTRACT

TAMPERE UNIVERSITY OF TECHNOLOGY
Master's Degree Programme in Science and Engineering
FANNI MYLLÄRI: Gas–particle equilibrium of alkali metal compounds studied in an aerosol test reactor
Master of Science Thesis, 45 pages, 3 Appendix pages
December 2013
Major: Advanced engineering physics
Examiner: Professor Jorma Keskinen, Docent Topi Rönkkö
Keywords: gas–particle equilibrium, aerosol, alkali metal compounds, kraft recovery boiler, furnace, black liquor, fine particles

The research topic of this thesis is inorganic gases from combustion that form particles via gas-to-particle conversion. The particles formed in gas-to-particle conversion have an effect on fouling of the super heaters and corrosion in boilers. These are the main reasons for unscheduled shutdowns and tube failure. Aerosol particles formed from inorganic gases are challenging to study in boiler conditions. To be able to measure the particles formed via gas-to-particle conversion, the related processes need to be isolated from the boiler to a smaller and easily controllable environment.

The experiments of this thesis were conducted in laboratory environment. The most important facilities used were high-temperature chambers, particle sampling and particle instruments. The first high-temperature chamber is used for the vaporization of the reactants, and the latter is used to achieve the gas-to-particle equilibrium. Water solution of solid reactants is fed to the chamber in order to control the amount of reactants. In addition, different gases are fed to the chamber. The reactants used in this thesis were selected from black liquor recovery boiler process. Black liquor composition is highly affected by the quality of the wood used in pulping, and that is why the reactant concentrations should be controllable. Black liquor consists mainly of sodium and sulphur but also of chloride from the wood. The chloride has been observed to be problematic since it causes corrosion in recovery boilers. A sample was taken from the second high-temperature chamber by diluting it in three steps before the particle measurement equipment.

The measurement results show two mode particle size distributions. Results indicate that one of the mode is formed in high-temperature conditions and the other in the dilution. It was discovered that alkali sulphate formation is the key component of the particle formation in the second high-temperature chamber. Indirect references of alkali chloride formation are observed by studying the nucleation mode. The nucleation mode particle number is decreased when temperature of the second high-temperature chamber is lowered because more alkali chloride compounds is transferred to the particle phase already in high temperature conditions.

TIIVISTELMÄ

TAMPEREEN TEKNILLINEN YLIOPISTO
Teknis-luonnontieteellinen koulutusohjelma
FANNI MYLLÄRI: Alkalimetalliyhdisteiden kaasu–hiukkastasapainon tutkiminen aerosolitestireaktorissa
Diplomityö, 45 sivua, 3 liitesivua
Joulukuu 2013
Pääaine: Teknillinen fysiikka
Tarkastajat: Professori Jorma Keskinen, Dosentti Topi Rönkkö
Avainsanat: kaasu–hiukkastasapaino, aerosoli, alkalimetalliyhdisteet, soodakattila, uuni, mustalipeä, pienhiukkaset

Työn tutkimusaihe on polttoprosessissa syntyvien epäorgaanisten kaasujen kaasu–hiukkasmuuntumassa muodostuvat hiukkaset, jotka vaikuttavat voimalaitoskattiloissa esimerkiksi tulistimien likaantumiseen ja korroosioon. Nämä taas johtavat suunnittelemattomiin huoltotaukoihin ja putkivaurioihin. Epäorgaanisten kaasujen tuottamien aerosolihiukkasen muodostumisprosessi ja koostumus on haastavaa selvittää kattilaolosuhteissa. Kaasu–hiukkasmuuntuman mittaaminen luotettavasti vaatii hiukkasmuodostukseen vaikuttavien prosessien eristämisen voimalaitoskattilasta pienempään, helpommin hallittavaan ympäristöön.

Tämän työn mittaukset suoritettiin laboratoriossa. Mittalaitteiston tärkeimmät osat ovat korkean lämpötilan näytekammiot, sekä hiukkasten näytteenotto- ja mittalaitteet. Ensimmäinen kammiota käytetään lähtöaineiden höyrystämiseen, toista korkean lämpötilan näytekammiota kaasu–hiukkastasapainon saavuttamiseen. Kiinteät lähtöaineet syötetään kammioon vesiliuoksena, jotta aineiden määrä olisi helpommin kontrolloitavissa. Näiden lisäksi kammioon johdetaan erilaisia kanto- ja reagenssikaasuja. Tässä työssä käytettyjen lähtöaineiden määrät ovat valittu mustalipeän regenerointiprosessin perusteella. Mustalipeän koostumukseen vaikuttaa sellun keitossa käytetty puulaatu, joten lähtöaineiden määrien tulee olla muutettavissa. Mustalipeä sisältää natriumia ja rikkiä, joiden lisäksi puuaineksessa prosessiin tulee mukaan kloridia, joka on havaittu ongelmalliseksi ja korrosiota aiheuttavaksi. Näyte otettiin jälkimmäisestä kammiosta laimentamalla sitä kolmessa vaiheessa ennen hiukkasmittalaitteita.

Mittaustulokset osoittavat kaksihuippuisia hiukkaskokojakaumia. Jakauma on muodostunut kaasuhiukkasmuuntumalla korkean lämpötilan näytekammiossa, ja toinen huippu, vastaavasti laimennuksessa. Hiukkasmuodostuksen kannalta tärkein hiukkasia muodostava komponentti on alkalisulfaatti. Epäsuoria viitteitä alkalikloridien muodostumisesta oli havaittavissa tutkimalla nukleaatiomoodia, jonka hiukkasten lukumäärä pienenee lämpötilan pienentyessä toisessa korkean lämpötilan näytekammiossa, koska alkalikloridejа siirtyy hiukkasfaasiin.

PREFACE

The work of this thesis has been done in the Aerosol Physics Laboratory of the Department of Physics at Tampere University of Technology. I want to thank my supervisors, M. Sc. Tech. Panu Karjalainen from the Department of Physics and M. Sc. Tech. Aino Leppänen from the Chemistry and Bioengineering, for their guidance and support. I would like to thank Prof. Jorma Keskinen for giving me the opportunity to work in the Aerosol Physics Laboratory and for being one of the examiners of this thesis. Docent Topi Rönkkö is also worthy of my gratitude for being the other examiner and also for believing in me as I was finishing this thesis.

The research area are has been interesting, and it has offered me challenges. I want to thank Metso Power and especially Erkki Välimäki for giving me the opportunity to work with this topic. The study would not have been completed without the co-workers in the OQ group, present and former members. All of you have been very encouraging all the time. We have had interesting conversations both on and off the topic. Part of my gratitude belongs to the physics workshop. I have had some wild ideas for getting my measurement setup better, and you have carried out them all.

I also want to thank my friends in SBS Tamppi and Hiukkanen. You have kept me going and gave me other things to think about and new problems to solve.

None of this would have happened without my parents. Kiitos äidille ja isälle, jotka ovat rohkaiseet minua jo pienestä pitäen luonnontutkimukseen. Tämä kirja ei olisi tässä ilman teidän tukeanne. Osa kiitoksista kuuluu myös veljilleni Mikolle ja Artulle. And last but not least, my love, Markku. Thank you for your support and for believing in me as I was finishing this thesis.

Tampere 7.11.2013

Fanni Mylläri

CONTENTS

NOMENCLATURE

Symbol	**Quantity**
d_p	Particle diameter
d_p^*	Kelvin diameter
i	Number of ions
m	Mass
M	Molecular weight
M_s	Molecular weight of salt
M_w	Molecular weight of solvent
R	Universal gas constant
S_R	Saturation ration
T	Temperature
η	Viscosity
γ	Surface tension
ρ	Density of the fluid
ρ_p	Density of the particle

Abbreviations

DR	Dilution Ratio
EEPS	Engine Exhaust Particle Sizer
ELPI	Electrical low-pressure impactor
TSR	Total reduced sulphur gases
VOC	Volatile organic compound

1. INTRODUCTION

The chemical recovery system enables the reuse of chemicals in the paper pulping system. The reduction of chemicals is achieved by combusting the spent cooking chemicals, black liquor, in the recovery boiler. The chemical recovery processes, especially black liquor combustion, generates heat, which is converted to electricity (Tikka, 2008). Black liquor combustion produces inorganic gases, such as alkali chlorides, fly ash, unburned black liquor carryover particles, and normal combustion gases (e.g., H_2O, CO_2, NO_2) (Frederick, 1997). Combustion products originate from the pulping liquor whose composition is dependent on the used wood species. The used wood species affects the amount of chloride in the black liquor. Additionally, sodium and sulphur originate from the pulping chemicals (Vakkilainen, 2005).

There are challenges, such as corrosion, fouling, and slagging of boiler surfaces, which are caused by the deposition of fly ash, carryovers (unburned black liquor droplets), and particles formed from inorganic gases when combusting black liquor. Depositions of particles on surfaces can be formed in different ways, such as by the impaction of particles to surfaces, and the diffusion of particles or by thermophoresis caused by temperature gradients between high temperature flue gas and cooler boiler surfaces (Kulkarni et al., 2011a, Cameron and Goerg-Wood, 1999). Slagging and fouling of superheaters are some of the reasons for inefficiency in the energy production, and additionally, corrosion may cause tube failure and unscheduled shutdowns (Tran, 1997a,b).

In the Kraft recovery boiler, coarse particles, with diameters over 2.5 μm, play a crucial role in ash deposit formation because the deposition rate of coarse particles is higher than that of fine particles. Mikkanen et al. (2001) have studied the coarse particle mass fraction and types at the superheater area. They found out that the mass fraction of coarse particles is 40% of the total particle concentration. They also found five different particle types, according to, shapes of the particles. Typing of the particles was used to achieve information about the possible particle formation mechanisms. For example, some particles were enriched with potassium. Mikkanen et al. (2001) assumed that those particles were formed via vaporisation of carryovers. Mikkanen et al. (1999) have also studied alkali salt particle formation in recovery boilers. According to them, fine particle mode (particle under 2.5 μm) is formed via vapour condensation. The main component in fine particles was sodium sulphate.

Mikkanen et al. (1999) also found out that chloride in particles was bounded with sodium, instead of potassium.

The aim of this thesis was to build a high-temperature test reactor, in which the gaseous precursors and aerosol particle formation can be studied in a controlled environment. By controlling the particle forming substances and reactor temperature, different aerosol phenomena related to combustion processes involving alkali metals can be studied. The main focus of this study was to validate the reliability of the test reactor and to apply it in practice. The particle-forming substances were chosen from a black liquor combustion process where inorganic compounds can be in the vapour phase or in the particulate phase when the combustion products are cooled down in the flue gas. In this thesis, the particle formation via gas-to-particle conversion was studied with different temperatures, which were determined by the Kraft recovery boiler. The highest temperature was 1,000 °C, which corresponds to the Kraft recovery boiler furnace, and the lowest temperature was 500 °C in the superheaters. The purpose of the temperatures is to produce a gas-to-particle conversion that corresponds to that in a real Kraft recovery boiler. The information can be used to estimate the corrosive effect of the aerosol to superheaters and boiler surfaces.

There is no consensus of the corrosion mechanisms and reactions because the effect of the aerosol particles for the fouling, slagging, and chemical composition of deposits is unknown. Some of the aerosol particles are formed after the Kraft recovery boiler furnace, and the particle size distribution and the chemical composition of those particles is still unclear. One of the reasons for the lack of knowledge is that there has not yet been a way to measure the gas–particle equilibrium in a controlled environment.

2. CHARACTERISTICS AND PROCESSES OF AEROSOL PARTICLES

Seinfield and Pandis (2006) define aerosol as a suspension of fine solid or liquid particles in a gas. Depending on aerosol, they are usually stable from a few seconds to years. Also, the particle diameters varies a lot–from 0.002 μm to more than 100 μm (Hinds, 1999). Atmospheric particles arise from natural sources and from anthropogenic sources, such as sea spray and the combustion of fuels. Particles in the atmosphere can be divided into two groups: primary and secondary particles. Primary particles are emitted directly from the source, whereas particles which are formed in atmosphere by a gas-to-particle conversion process are called secondary particles (Seinfield and Pandis, 2006). In addition to atmosphere aerosol particles, some of the particles are from anthropogenic sources–e.g., power plants and diesel engines. Aerosol particles are also exploited in various fields–e.g., pharmaceutical, nanotechnology, and chemical manufacturing.

Particle size is one of the most important parameters when describing the behavior of aerosols. Each of the properties of an aerosol particle depends on the particle size–for example terminal velocity of the particle or the density of particle (Hinds, 1999). There are different definitions for particle diameter for different purposes–for example, an aerodynamic diameter is used in low-pressure impactor measurements. Thus, the appropriate particle size definition depends on the measurement method (Kulkarni et al., 2011b).

2.1 Particle formation and growth

'Aerosols, by their nature, are somewhat unstable in a sense that the concentration and particle properties change with time'(Hinds, 2011). These changes can be caused by external forces or chemical and physical processes that change the particle size or composition(Hinds, 2011). This chapter introduces the most significant mechanisms affecting the particle concentration, size, and composition: nucleation, condensation, and coagulation.

The vapour pressure or saturation vapour pressure is a unique property of any liquid in a known temperature. The saturation vapour pressure is the minimum partial pressure that the vapour of liquid that has to be to maintain the gas-liquid equilibrium in the gas-liquid interface to prevent evaporation. Normally, saturation

vapour pressures are determined for flat liquid surfaces, but in the case of aerosols, the liquid surface is curved, which has to be taken into account. When studying condensation and evaporation processes, we can see that the ratio of the partial pressure of vapour and the saturation vapour pressure is important. The ratio is called the saturation ratio, S_{R}, or relative humidity in the case of water(Hinds, 2011).

The saturation ratio is defined as a partial pressure required for mass equilibrium for a flat surface. For the curved surface of a liquid aerosol particle, the partial pressure has to be higher to maintain the mass equilibrium at a given temperature. This effect is called the Kelvin effect (2.1).

$$S_R = \exp\left(\frac{4\gamma M_{\mathrm{w}}}{\rho_{\mathrm{p}} R T d^*}\right) \tag{2.1}$$

In equation 2.1, γ (N m^{-2}) is surface tension, M_{w} (kg mol^{-1}) is the molecular weight, ρ_{p} (kg m^{-3}) is the density of the liquid particle, R (J K^{-1} mol^{-1}) is the gas constant, d^* (m) is the Kelvin diameter of the particle, and T (K) is the temperature. If the saturation ratio is greater than that required by the Kelvin equation, then the condensation and growth of particles are possible; otherwise, the particle evaporates or stays in the equilibrium size. If there are enough large particle clusters (from particles formed in the homogeneous nucleation), that have a diameter larger than the Kelvin diameter, the clusters begin to grow by condensation to larger particle sizes(Hinds, 2011, 1999).

Nucleation or nucleated condensation refers to the process of the initial formation of a particle from vapour. Nucleation can be divided in four types of nucleation processes based on the vapour and condensation nuclei:

1. homogeneous–homomolecular
2. homogeneous–heteromolecular
3. heterogeneous–homomolecular
4. heterogeneous–heteromolecular. (Seinfield and Pandis, 2006)

Types 1 and 2 nucleation are also called self-nucleation because particles are formed from one or more species of supersaturated vapour without the assistance of condensation nuclei or ion. When low vapour pressure substance exists in high supersaturation, those vapours can form particles by type 1 nucleation. The nucleation of types 1 and 2 require large saturation ratios; therefore they are normally observed in laboratory circumstances or chemical process situations(Hinds, 2011, 1999).

Type 3 nucleation occurs when single supersaturated vapour nucleates on a foreign surface. In type 4, nucleation takes place between two or more species on foreign substances. Types 3 and 4 nucleations are more common in comparison with types 1 and 2. The condensation nuclei present at the heterogeneous nucleation can be passive or active. A passive nucleus is insoluble, for example, in water. On the contrary, in sodium chloride (with a strong affinity to water), particles are soluble in water and therefore, the particles are formed more easily. The active soluble nucleus stabilizes the particle, whereas the Kelvin effect increases the equilibrium vapour pressure required over the particle surface (see equation 2.2). In equation 2.2, m (kg) is the mass of soluble salt, which has a molecular weight of M_s (kg mol^{-1}), M_w (kg mol^{-1}) is the molecular weight of the solvent, ρ (kg m^{-3}) is the density of the solvent, i is the number of ions each molecule of salt forms, and d_p (m) is the particle diameter. The growth after the Kelvin diameter particle size has been reached is called condensation, where vapour molecules stick at the particle surface(Hinds, 1999, Seinfield and Pandis, 2006, Hinds, 2011). If the nucleation or condensation increases the aerosol mass concentration, it is said that the particles are formed via gas-to-particle conversion.

$$S_R = (1 + \frac{6imM_\mathrm{w}}{M_\mathrm{s}\rho\pi d_\mathrm{p}^3})^{-1} \exp(\frac{4\gamma M_\mathrm{w}}{\rho_\mathrm{p} RT d_\mathrm{p}}) \tag{2.2}$$

Jensen et al. (2000) have studied the kinetics of the homogeneous nucleation of the pure chloride vapour at high temperatures. The study was made in a laboratory-scale tubular reactor with a laminar flow of synthetic flue gas. The synthetic flue gas was made by mixing N_2, O_2, and SO_2 with a water addition from another gas line. Alkali compounds were added with porous pellets. Jensen et al. (2000) found out that the chloride contributions are unlikely due to the formation of new particles. Jensen et al. (2000) also made measurements with extra SO_2 in the presence of oxygen and water vapours. It increased the number concentration of the flue gas particles and affected the composition of the particles by increasing the sulphate content in addition to chloride. According to their study, alkali sulphates are formed in the sulphation of vapour phase, rather than in solid, alkali chloride. 'The sulphate vapours are formed in high supersaturation and show a pronounced tendency towards homogeneous nucleation, which is identified as the likely source of the submicron particles formed in alkali rich flue gases'(Jensen et al., 2000).

As in the study of Jensen et al. (2000), sulphate vapour is the key substance that contributes to the growth of particles. In the study of McKeough and Janka (2001), focusing on sulphur behaviour in recovery boiler furnaces, sodium sulphate is assumed to be in a molten state in the lower and middle furnace temperature, so that the condensation to a surface of the sodium sulphate particle is possible. Potassium

sulphate and alkali chlorides condense to the sodium sulphate particle at lower temperatures than McKeough and Janka (2001) assumed. However, McKeough and Janka (2001) proposed that the potassium sulphate and alkali chloride condensation mechanism do not play a significant role in recovery furnace aerosol formation.

Coagulation is an aerosol process in which the aerosol particles collide and form a larger particle. The collisions between particles can be driven by a Brownian motion, then the coagulation process is called thermal coagulation. The collision can also be caused by hydrodynamic, electrical, gravitational, or other forces, in which cases the collision is called kinematic coagulation. Thermal coagulation resembles condensation of vapours, except that in the thermal coagulation, the particles' diffusion drives the particles to collide with each other. In coagulation processes, the supersaturation at the particle surface is not necessary for the particle diameter growth. The process is irreversible. As the result of coagulation, the number concentration of the particles decreases and the average particle size grows, while the mass or volume concentration does not change(Hinds, 2011, Seinfield and Pandis, 2006). The term 'coagulation' is addressed with liquid particles; in the case of solid particles, it is often called agglomeration. Agglomeration refers to particles that do not merge but that stick together as particle clusters via a Van Der Waals interaction. Particle shape is influenced by coalescence (sintering), where the particles in agglomerate fuse together, forming solid particles at high temperatures (Hinds, 1999).

Figure 2.1 shows the possible particle formation mechanisms at a high temperature environment. At a high-temperature environment, particle forming substances are in the vapour phase. When the temperature decreases, vapours can nucleate (lower path), as explained earlier, or condensate over nucleated seed particle (upper path). Small, nucleated particles or cluster(s) can then agglomerate or coagulate with each other or with the condensate particles. Agglomeration, condensation, and coagulation will have an effect on the particle population after approx. 100 nm. Condensation and nucleation processes can go backwards, which means that the compounds evaporate from the particle surface back to the gas phase. In general, evaporation requires an increase in temperature for a significant decrease of vapour pressure of gaseous phase.

2.2 Coarse particles

Coarse particles are defined as particles with diameters that are greater than 2.5 μm. These particles are formed by mechanical processes, and they can consist of human-made and natural dust particles(Seinfield and Pandis, 2006).

In recovery boiler processes, coarse particles play a crucial role in ash deposit formation. The coarse particle deposition rate is higher than that of fine particle deposition. Mikkanen et al. (2001) have studied the coarse particle mass fraction and

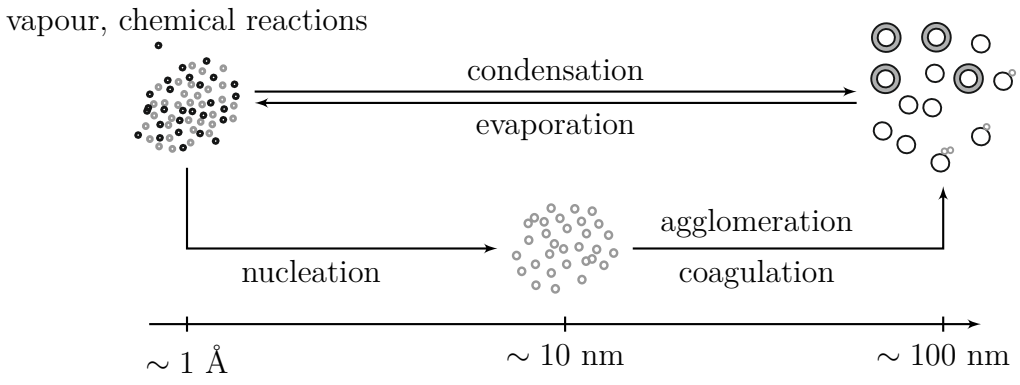

Figure 2.1: Particles form via nucleation and become larger via vapour condensation on particle surfaces. Formed particles can coagulate, agglomerate, or sinter to become larger. Particle diameter can change in condensation and evaporation processes.

the coarse particle types from samples taken from the superheater area of industrial recovery boiler. They found five different coarse particle types:

1. Partially sintered large agglomerates formed from fine fume particles that had been entrained from heat exchanger surfaces.

2. Extensively sintered irregular particles that had been entrained from the surfaces by soot blowing.

3. Spherical particles that appeared highly porous inside.

4. Dense spherical particles.

5. Intermediate irregular particles of non process mineral matter.

They (Mikkanen et al., 2001) assumed that type 3 particles were formed via vaporisation of carryovers because particles were enriched with potassium. Carryovers are small, black liquor droplets, which are entrained unburned into the flue gases and may burn in the upper furnace (Mikkanen et al., 1999). They found silicon and calcium in the type 5 particles, and traces of magnesium were also found. They suggested that those originate from the mineral impurities in the black liquor. Type 1 particles are most likely formed from fine fume particles. 'The similarity in the EDX spectra of the type 2 and type 1 particles, and the appearance of these particles indicate that they are formed by deposition and subsequent sintering of mainly fine fume particles on the heat exchangers', (Mikkanen et al., 2001). Type 4 particles might be sintered type 2 particles or mechanically ejected/fragmented salt residues.

2.3 Fine particles

The fine particle diameter is below 2.5 μm. 'Nucleation mode consists primarily of combustion particles emitted directly into the atmosphere and particles formed by gas to particle conversion' (Hinds, 1999). The particle number concentration is high near the nucleation particle source/formation; therefore coagulation might be significantly reducing the amount of particles at that point. Nucleation particles have a relatively short lifetime before ending up in the accumulation mode. Accumulation mode exists because of the weak removal mechanism of the particles. Removal mechanisms of the particles are rainout or washout, but the coagulation rate is too slow to reach the coarse particle mode. The nucleation and accumulation modes constitute the fine particles (Hinds, 1999).

3. KRAFT RECOVERY BOILER

In paper pulping process the wood chips are boiled with cooking chemicals, such as sodium sulphide and sodium carbonate. Chemical pulp is used in paper production, while the spent cooking chemicals (black liquor) are recovered in a recovery boiler. The chemical recovery system was introduced in the 1930s and 1940s. Before that, the spent cooking chemicals were discarded. Black liquor recovery has a few advantages. First, the combustion of black liquor releases energy to generate steam and electricity, so more energy can be produced than is needed in the recovery cycle. Second, the recovery cycle makes possible the reuse of cooking chemicals. The main components of the Kraft recovery process are: the evaporation of water from black liquor, the firing of black liquor in a recovery furnace to gain energy to recover the sodium sulphide and sodium carbonate in the char bed, the causticizing of sodium carbonate to the sodium hydroxide, and the regeneration of lime mud in a lime kiln. Other minor operations concerning the pulping processes are, for example, the removal of soap and adding of make-up chemicals (Na_2S, Na_2CO_3) to the mixing tank. There are also some procedures concerning removal of odorous gases, chlorine, and potassium (Tikka, 2008).

Figure 3.1 shows a cross-section of a recovery boiler. It consists of superheaters (primary I, primary II, secondary, and tertiary), an economizer, a boiler bank, screen tubes, and a lower furnace. In the next few paragraphs, I will introduce some processes concerning the Kraft recovery process.

Evaporation of water in black liquor is used to rise the black liquor concentration with minimum chemical losses. The evaporation of black liquor has three different operations. First is the separation of water from black liquor to generate, concentrated black liquor and condensate. Secondly, the condensate is processed to segregate clean and fouled condensate fractions. Thirdly, the soap is separated from the black liquor. The soap is formed via the reaction of the acetyl group in hemicellulose and sodium hydroxide (Tikka, 2008).

For combustion, the black liquor is sprayed into the furnace through a number of liquor guns (Figure 3.2, p. 10). The reason for this is to produce small droplets to maximize the temperature and combustion. When burning the black liquor droplets, the organic matter combusts fully, while the inorganic portion partially vapourises and reacts in the furnace, producing fumes. The inactive portion of the black liquor

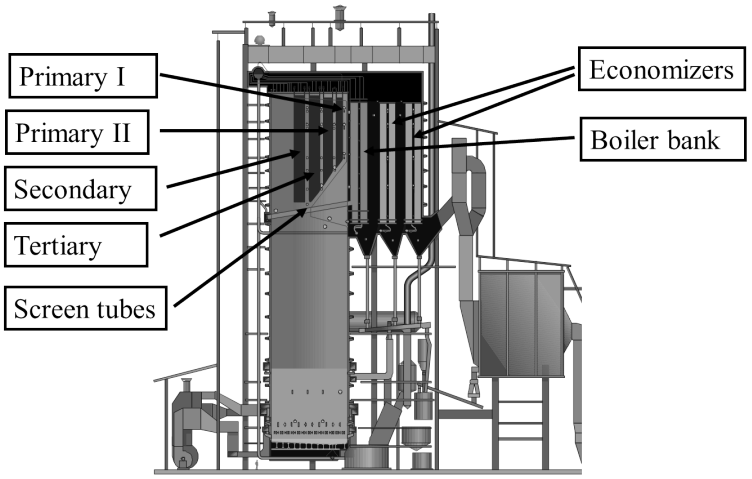

Figure 3.1: Kraft recovery boiler (TAPPI, 2001).

passes through the system without participating in the combustion process (Adams, 1997, Vakkilainen, 2005, Tikka, 2008).

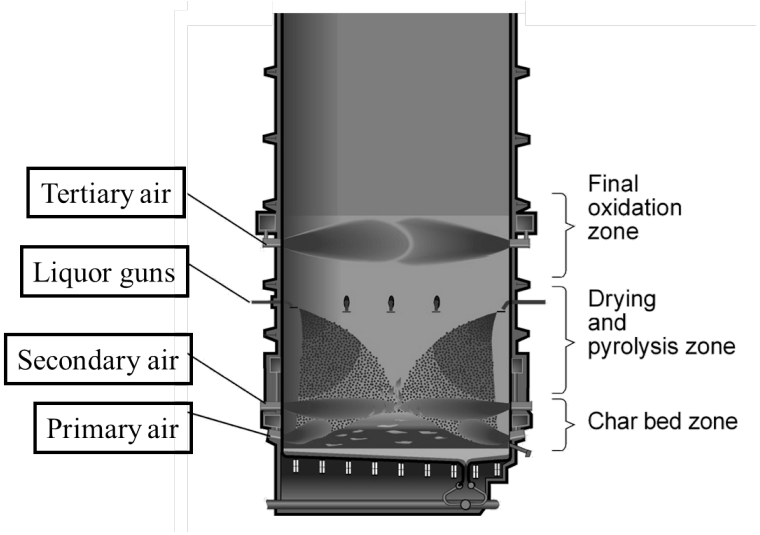

Figure 3.2: Kraft recovery boiler's lower furnace (TAPPI, 2001).

In the lower furnace, the char bed, the inorganic sulphur compounds are reduced to sodium sulphide. The molten inorganic part, smelt, mostly consisting of alkali salts, (Na_2S, Na_2CO_3) is collected for reuse. Smelt is collected for further use through smelt spouts (Figure 3.2, p. 10). From smelt spouts, it is sprayed over-pressurized to the dissolving tank, where it dissolves in weak white liquor from the lime mud washing process. Mixing smelt and weak white liquor produces raw green liquor, which goes to a recausticizing plant for clarification and causticizing.

(Adams, 1997, Vakkilainen, 2005, Tikka, 2008)

Lime kiln (reaction 3.1) is used to calcine lime mud ($CaCO_3$) to reactivate lime (CaO) by drying and heating. Calcining processes are endothermic and therefore require heat, which is produced by burning oil or natural gas in the lime kiln. Causticizing processes use the green liquor, formed from white liquor and smelt. Green liquor is clarified and filtrated before further use. After filtration and clarification, the green liquor is mixed with lime. When water in green liquor reacts via reaction 3.2, the process is called slacking. After slacking, the formed calcium hydroxide reacts with sodium carbonate to form sodium hydroxide and lime mud ($CaCO_3$). The causticization reaction is presented in reaction 3.3. The lime mud is separated and washed, while the white liquor is filtrated and clarified (Tikka, 2008, Puhakka and Tolonen, 2007).

$$CaCO_3\ (s) \rightarrow CaO\ (s) + CO_2\ (g) \tag{3.1}$$

$$CaO\ (s) + H_2O\ (l) \rightarrow Ca(OH)_2\ (s) \tag{3.2}$$

$$Na_2CO_3\ (aq) + Ca(OH)_2\ (s) \rightarrow 2\ NaOH + CaCO_3\ (s) \tag{3.3}$$

3.1 Black liquor properties

Black liquor is a complex mixture of water, inorganic oxidized salts from white liquor (Na_2SO_4, NaCl, Na_2CO_3,$Na_2S_2O_3$, NaOH and Na_2S), and organic matter. The pulping process consumes most of the sodium hydroxide in the neutralization of the wood acids. Part of the sodium sulphide oxidizes in the pulping to sodium tiosulphate. Hydroxide and hydrosulphide ions in Kraft white liquor contribute to lignin degradation. Hydroxide ions also dissolve polysaccharides in wood (Vakkilainen, 2005). Black liquor properties are entirely defined by the wood species, the cooking method, white liquor and the pulping process. (Vakkilainen, 2005). The weak black liquor concentration of dry solids in water is 15%, but it is concentrated in the evaporation processes to 65% to 85% dry solids content for the firing. Liquor viscosity may change for more than two orders of magnitude through the liquor loop only because of water vaporization. The alkali constituents in the white liquor (NaOH and Na_2S) and black liquor are important for the processes. High alkali content in the white liquor during pulping enhances the dissolving of lignin and polysaccharides to the pulp from the wood. Therefore, lignin and polysaccharides are easily entangled, even though they degrade faster. At shorter pulping times higher alkali content also increases the liquor viscosity because the pulp lignin concentration does not change. Residual alkali (also know as effective alkali NaOH,

$\frac{1}{2}Na_2S$) has an effect on the liquor viscosity, and higher alkali content yields lower viscosity; however if the alkali content is too high, the viscosity can increase again (Adams, 1997, Frederick, 1997, Vakkilainen, 2005).

Table 3.1 lists the typical compositions of virgin black liquor, which is black liquor before water evaporation. As stated earlier, the composition of black liquor varies with the wood quality and the pulping liquor. North American hardwood contains more carbon than Nordic hardwood. Nordic softwood contains the least similar amount of carbon compared with softwood and North American hardwood. From Table 3.1, it can be seen that the oxygen content of Nordic softwood is the lowest. It is also remarkable that the amount of sulphur varies drastically between Nordic and North American wood. North American softwood has the lowest potassium content.

Table 3.1: Typical composition of virgin black liquor (black liquor before water evaporation) from Nordic (N) and North American (NA) wood. Softwoods are pine, and the Nordic hardwood is birch, while the North American hardwood has not been identified (Tikka, 2008).

	Softwood (N)	Hardwood (N)	Softwood (NA)	Hardwood (NA)
Carbon, %	35.0	32.5	35.0	34.0
Hydrogen, %	3.6	3.3	3.5	3.4
Nitrogen, %	0.1	0.2	0.1	0.2
Oxygen, %	33.9	35.5	35.4	35.0
Sodium, %	19.0	19.8	19.4	20.0
Potassium, %	2.2	2.0	1.6	2.0
Sulphur, %	5.5	6.0	4.2	4.3
Chlorine, %	0.5	0.5	0.6	0.6
Inert, %	0.2	0.2	0.2	0.5

3.2 Combustion of a black liquor droplet and char bed processes

The surface area of the black liquor needs to be increased to gain efficient combustion and reduction of chemicals. Therefore, the black liquor is sprayed into droplets. Black liquor droplets are from 0.5 to 5 mm in diameter. The droplet burning has five different stages: drying, devolatilization, char burning, smelt coalescence, and reactions, of which the devolatilization of the black liquor droplet is the most interesting. The devolatilization process is called pyrolysis, which is a non-oxygen process. In the case of recovery boilers the pyrolysis is actually a low-oxygen process. The droplet swells, and the organic material breaks down into tar. The tar decomposes into gases and light hydrocarbons–e.g. CO_x, H_2, H_2O, H_2S, NO, and NH_3. Most of the flue gas elements are released at this stage, including sodium, potassium, and sulphur gases. About half of the black liquor solids are volatilized during devolatilization. The swelling of the black liquor droplet changes the internal

and external transport process around the droplet, and it can also present a dramatic change to entrainment to flue gas. Particle swelling increases the surface area of the droplet and the porosity, which enhances reactivity. After devolatilization, the remaining organic char is burned, and the inorganic salts in the char bed hasten the burning rate. What is left of the black liquor droplet is inorganic salts, smelt (Frederick and Hupa, 1997).

The char bed (see Figure 3.2) consists of carbon, partially pyrolyzed black liquor solids, and molten and cold smelt. Typically, the combustion residues cover the whole floor area of the furnace. In an ideal situation, the inorganic pulping chemicals are separated from the burning char. The pulping chemicals are in a molten and reduced state while flowing out of the smelt spouts. The char bed is used to provide a reducing environment for the sulphide in molten smelt to prevent the sulfide reoxidizing to sulphate. The char bed size and shape are determined by the boiler design, firing technique, air delivery, and the black liquor combustion properties. Normally, the char bed consists of a few layers. The bottom layer is unreactive and supports the upper layer, where the char burns actively. Between the active layer and the passive layer is a dense and chemically inactive core of a bed. The largest black liquor droplets normally reach the bed without drying entirely or being completely devolatilized. Smaller droplets, on the other hand, may be partially or completely burned before reaching the char bed (Grace and Frederick, 1997).

Sulfate reduction reactions in the char bed are presented in reaction equations 3.4, 3.5, and 3.6. The reactions 3.5 and 3.6 occur rapidly. The rate of sulphate reduction with carbon monoxide (reaction 3.7) is more than two orders of magnitude slower than that with carbon at the char bed (see reaction 3.7). The reduction is dependent on the temperature. Fine particles can increase the possibility of sulphide reoxidation. Too-small particles burn too quickly and deplete the carbon before the total reduction of the sulphate has happened in the particle. If the particle is then exposed to combustion air, which leads to unwanted reoxidation of sulphide to sulphate (Grace and Frederick, 1997).

$$2\ O_2\ (g) + Na_2S \rightarrow Na_2SO_4 \tag{3.4}$$

$$Na_2SO_4 + 4\ C \rightleftharpoons Na_2S + 4\ CO\ (g) \tag{3.5}$$

$$Na_2SO_4 + 2\ C \rightleftharpoons Na_2S + 2\ CO_2\ (g) \tag{3.6}$$

$$Na_2SO_4 + 4\ CO \rightleftharpoons Na_2S + 2\ CO_2\ (g) \tag{3.7}$$

Table 3.2: Melting (MP) and boiling (BP) points for alkali metal compounds, which can be formed in Kraft recovery boiler. If BP is not known, it is marked with - (Sigma Aldrich, 2011).

Compound	MP (° C)	BP (° C)	ρ (g cm^{-3})
NaCl	801	1413	2.160
KCl	770	1500	1.980
HCl	-30	100	1.200
NaOH	318	1390	2.130
KOH	361	1320	2.044
Na_2SO_4	884	-	2.680
K_2SO_4	-	-	2.662
Na_2CO_3	851	-	2.532
K_2CO_3	891	-	2.428

3.3 Gaseous compounds and possible reactions in a Kraft recovery boiler

The main components of the flue gas from black liquor combustion are water vapour, oxygen, carbon monoxide, carbon dioxide, sulphur dioxide, TSR (total reduced sulphur gases), and nitric oxides (Vakkilainen, 2005). General interest has changed to gases, such as HCl, NH_3, CO, methanol, and other VOC emissions (Tran and Vakkilainen, 2008). In this thesis, the main focus is on the reactions in the lower furnace. In the lower furnace, the main gases are hydrogen, water, carbon monoxide and dioxide, oxygen, nitrogen, methane, hydrogen sulphide, sodium, sodium hydroxide, and sodium chloride (Vakkilainen, 2005). Table 3.2 lists the possible reaction products of inorganic gases reacting in the Kraft recovery boiler furnace.

Sodium and potassium are chemically related; therefore, they are discussed together. Potassium compounds are much more volatile than sodium compounds. Therefore, potassium is also enriched in the dust (Hupa, 1997). All of the sodium compounds can also be found as potassium compounds, so all Na's can be replaced with K's in the reaction equations. The sodium content of black liquor is around 20 w-% and that of potassium is 3-5 % of black liquor. (Vakkilainen, 2005)

Sodium is released in black liquor combustion and char bed reaction through the vaporization and reduction of sodium carbonate. The release of sodium is a function of temperature, so the increase in temperature increases the release of sodium. It has also been noticed that the amount of electrostatic precipitator dust is linked to the release of sodium (Vakkilainen, 2005).

The flue gas chemistry has been studied by McKeough and Vakkilainen (1998) via chemical-equilibrium calculations. They claim that in the recovery boiler at the

tertiary air area, sodium as well as potassium hydroxide react with sulfur dioxide and oxygen, producing sulphate compounds via 3.8. McKeough and Janka (2001) claim that the 3.8 in the gas phase is the primary sulphur-capture reaction, which leads to the formation of alkali sulphate fume particles.

$$2\ \mathrm{NaOH} + \mathrm{SO_2}\ (\mathrm{g}) + 0.5\ \mathrm{O_2}\ (\mathrm{g}) \rightarrow \mathrm{Na_2SO_4} + \mathrm{H_2O}\ (\mathrm{g}) \tag{3.8}$$

In McKeough and Janka (2001), the reaction 3.8 is considered to occur in the gas phase so that the alkali sulphates formed are initially in gaseous form. Therefore, the fume formation can begin in the lower furnace, and the fume formed mainly comprises alkali sulphates. The reaction (3.8) is considered the most important. The reactions presented below are also possible in the Kraft recovery boiler. Reaction 3.3 is possible, according to Vakkilainen (2005).

$$\mathrm{NaOH} + \mathrm{NaHSO_4} \rightarrow \mathrm{Na_2SO_4} + \mathrm{H_2O}\ (\mathrm{g}) \tag{3.9}$$

The sodium hydroxide might react with carbon dioxide, producing sodium carbonate and water vapour (3.10). It is known that the sodium carbonate decomposes at high temperatures; therefore the reaction 3.10 is an equilibrium reaction (Mikkanen et al., 1999). The decomposition of Na_2CO_3 is possible in high temperatures above 1,300 °C, according to Mikkanen et al. (1999). In Jokiniemi et al. (1996), reaction 3.10 is more likely to form Na_2CO_3 on the particle surface.

$$2\ \mathrm{NaOH} + \mathrm{CO_2}\ (\mathrm{g}) \rightleftharpoons \mathrm{Na_2CO_3} + \mathrm{H_2O}\ (\mathrm{g}) \tag{3.10}$$

$$\mathrm{Na_2CO_3} + \mathrm{SO_2}\ (\mathrm{g}) + 0.5\ \mathrm{O_2}\ (\mathrm{g}) \rightarrow \mathrm{Na_2SO_4} + \mathrm{CO_2}\ (\mathrm{g}) \tag{3.11}$$

In Eskola et al. (1998), the most probable sodium containing gaseous components in the lower furnace are sodium chloride and sodium hydroxide, whereas potassium compounds in the lower furnace are K and KOH. If there is enough chloride, also KCl can be found in the flue gas (Hupa, 1997).

Sulphur emissions, such as sulphur dioxide, have decreased from 500 ppm in the 1970s close to zero in modern boilers (Mikkanen, 2000). The sulphur in black liquor is mainly in inorganic compounds, such as sulphide and sulphate. Elemental sulphur is not a stable compound in recovery furnace conditions, and it has been claimed that about 30% of incoming sulphur is released from a recovery boiler furnace in the flue gas and fume. The sulphur release depends on the amount of dry solids of a black liquor. At high dry solid, there is hardly any gaseous SO_2 leaving the boiler (Vakkilainen, 2005). In this thesis, the sulfur is fed as SO_2 gas to the test reactor.

The possible reactions leading to lower the SO_2 emissions are 3.3 and 3.11.

In a recovery boiler furnace, there are gaseous Na and K. These gases react with SO_2 or Cl, producing sulphate or chloride fumes, which are more stable than carbonate (Na_2CO_3, K_2CO_3) fumes. If there is not enough sulphur or chloride, the fume condenses as carbonates (Kochesfahani, 1999).

On the other hand, McKeough and Janka (2001) claim that the reaction 3.10 can occur on the particle surface because the carbonate compounds cannot be found in a gas phase. Therefore, the hydroxides have to be condensed on the particle surface to enable reaction 3.10. In the absence of SO_2, reaction 3.10 is thermodynamically favoured. However, if the flue gas contains SO_2 when the alkali hydroxides condense, the reaction is thermodynamically favoured. When all alkali hydroxides and most of the SO_2 have reacted, the sulphur capture reaction is 3.11. But reaction 3.11 can be observed at low furnace temperatures and/or in the presence of poor mixing.

Chlorine occurs in the lower part of the furnace almost solely as NaCl and KCl gases. The vapour pressure of these gases is higher than those of other sodium and potassium compounds. Therefore, the chlorine compounds are enriched into a gas phase in the furnace. Chlorine can exist in the furnace gases, and in the smelt, the distribution is strongly temperature-dependent. At high temperatures, most of the chloride is in the vapour phase. Sodium release is thermodynamically limited, and potassium release is considered to be similar to sodium release–at least, they have some kind of dependency. Chloride release is not limited thermodynamically and, therefore, high chloride content can be found in the particles (Hupa, 1997, McKeough, 2010).

As the flue gas cools down, the vaporized chloride starts to condense into dust. Small amounts of condensed chloride essentially change the behavior of the flue gas dust in the flue gas duct. Chlorate compounds, especially potassium chloride, lower the dust melting temperature range, resulting in the dust being stickier and more fouling (Hupa, 1997).

$$2\ \mathrm{NaCl\ (g,c)} + \mathrm{SO_2\ (g)} + 0.5\ \mathrm{O_2\ (g)} + \mathrm{H_2O\ (g)} \rightarrow \mathrm{Na_2SO_4\ (c)} + 2\ \mathrm{HCl\ (g)} \quad (3.12)$$

Hydrochloric acid is formed as a result of sulphation of alkali chlorides (NaCl and KCl, see equation 3.12) if SO_2 concentration is high and if there is enough chloride in the black liquor. Formation of hydrochloric acid can be reduced with high bed temperature and by minimizing the SO_2 concentration in the flue gas (Tran and Vakkilainen, 2008). The S/Na_2 ratio is a significant parameter due to chloride chemistry (Hupa, 1997).

Of all the individual flue gas components, potassium chloride has the lowest melting point of 770 °C. Therefore, it is in contradiction to the fact that the majority of the solid fumes start forming when the flue gas temperature is 550-650 degrees (Tavares and Tran, 1997). The fume formation has only been noticed in Tavares and Tran (1997). Along with McKeough and Vakkilainen (1998), the conclusions of Tavares and Tran (1997)'s research are made poorly; also, the measurement technique collects some criticism. Neither have the gas flow velocities inside the probe been high enough nor have the temperature gradients been studied.

3.4 Corrosion and fouling

Corrosion is a problem from the bottom of the furnace all the way up to the top and to the electrostatic precipitator. It can be found in different forms: sulphidation, thermal oxidation, stress corrosion cracking, molten salt corrosion, pitting corrosion, erosion corrosion, aqueous corrosion, and dew point corrosion. Corrosion can cause tube failure, which can lead to an unscheduled boiler shutdown (Tran, 1997a).

A heat transfer tube is exposed to corrosive gases, liquid, or deposits. In normal conditions, the tube surface is coated with a layer of deposits, which corrosive gases must pass in order to affect the tube surface. Gas phase corrosion dominates the tube thinning, if the tube's surface temperature is lower than the deposit first melting temperature, and the temperature or the concentration of corrosive gases is high enough. If the tube temperature is higher than the deposit first melting temperature, liquid phase corrosion is dominant. The molten or partially molten deposit increases the corrosion rate. On the other hand, the deposit may decrease the rate of the corrosion by slowing down the diffusion of the corrosive substance to the tube surface (Tran, 1997a).

The most corrosive gases are S- and Cl-bearing gases, even though they are minor components of the flue gas. In a boiler, the concentrations vary greatly with location, local atmosphere (oxidizing or reducing), the temperature, and the degree of mixing in the flue gas. Acidic sulphur gases (SO_2, SO_3, H_2SO_4) are a result of total oxidation of sulphur. These gases should not have an effect on the corrosion in the lower furnace. In the upper furnace, the sulphur gases contribute to the formation of acidic sulphates ($Na_2S_2O_7$, $NaHSO_4$). These alkali sulphates are responsible for the pitting corrosion and the tube thinning in the generating bank and economizer regions. Gases also cause acid dew point corrosion. Another corrosive gas is hydrogen chloride (HCl). In the lower furnace, the amount of hydrogen chloride gas is not important. The concentration of hydrogen chloride is higher in the upper furnace due to reaction 3.12 (Tran, 1997a).

Skrifvars et al. (2008) have studied the effect of alkali salt deposit composition on the corrosion of superheater steel. They tested the materials in temperatures

between 400-600 degrees by making synthetic alkali salt deposits. The result was that the increased amount of melt in the salt deposit increased the corrosion. The test also showed that chloride salt had a corrosive effect at lower temperatures.

Particle deposition decreases the heat transfer efficiency of the boiler, which causes a lower superheated steam production rate and/or reduced steam temperature and pressure. Deposits can also form a locally corrosive environment, which may damage tubes. Flue gas flow can be examined in two different ways. The first way is the microscopic level where each particle modifies the gas flow over and around the superheater tube through its own physical properties. Another way to examine the flue gas flow is at the macroscopic level. The macroscopic level considers the gas flow characteristics that may determine the particle transportation and the deposition on the surface. In the next few paragraphs, I will introduced the basic particle motions that have an effect on deposition formation. Five basic particle motions are: molecular diffusion, Brownian diffusion, turbulent diffusion, thermophoresis, and inertial impaction (Tran, 1997b, Kulkarni et al., 2011a). Vapour or gaseous species can condense on the surfaces and react with deposits (Vakkilainen, 2005).

The random movement of gas molecules causes gas and particle diffusion if there is a concentration gradient. Diffusion always causes a net movement of compounds from higher concentration to lower concentration. Excluding convection, the thermal diffusion is limited to particles smaller than 0.1 μm. The thermal diffusion is mainly the same as Brownian motion (particle diffusion). Compared to thermal diffusion, the Brownian motion is dominating the diffusion for a larger particle motion. Larger particles have larger inertia and large surface area over for the gas molecules to bomb the surface; therefore, the larger particles diffuse more slower than the smaller ones (Kulkarni et al., 2011a, Hinds, 1999, Tran, 1997b).

There are three different types of turbulent diffusion. The first type is in a turbulent diffusion regime, where the turbulence influences central mixing, and Brownian diffusion is the mechanism whereby particles are transported through the laminar sub-layer to the tube wall. This regime is related to the small particles. The second type is in turbulent diffusion -eddy impaction regime, which applies to larger particles and where inertia is remarkable. In the second regime particle deposition increases with increasing particle size. The third type is in particle inertia, a moderated regime that is suitable for large particles. The particle inertia is large so that the particle trajectories are less affected by the turbulence; therefore, the turbulent inertial depositions decrease slightly with increasing particle size (Brockmann, 2011).

Thermophoresis is caused by a thermal gradient. In thermophoresis, particles are being bombarded more strongly from the hotter side and therefore forced away from a heat source. Thus, heated surfaces are often clean while relatively cool surfaces

tend to collect particles. For particles smaller than the mean free path, the thermophoretic velocity is independent of the particle size. For particles bigger than the mean free path, the thermophoretic velocity depends on the thermal conductivity of the gas and the particle size. The thermal conductivity decreases the thermophoretic velocity (Kulkarni et al., 2011a, p. 27-28).

In a recovery boiler, there are two basic kinds of deposits formed by fly ash particles. Fly ash particles that cause deposit are carryover particles and fumes. A fume is an aerosol, which consists of solid particles in gas, whereas the carryover is a small black liquor droplet, which has plunged to flue gas instead of a char bed. Fume and carryovers can form deposits on the tube surface in the upper boiler. Carryover deposits are formed by impaction on the tube surface. Fume particle deposits can be formed directly to a cooled surface or indirectly forming particles in the flue gas, which then are transferred to the cool surfaces by thermophoresis or turbulent diffusion. Fume deposits are usually white or soft unlike carryover deposits, which are pink, fused, and very hard (Tran, 1997b). Cameron and Goerg-Wood (1999)'s experimental results showed that thermophoresis is the dominant mechanism for fume deposition under conditions similar to those in the Kraft recovery furnace.

Recovery boiler deposits have two different melting temperatures. The first temperature is the one where the material begins to melt. Below the temperature there is no liquid phase. At the second temperature, the material is totally molten. Between these two temperatures can be found two other important temperatures: sticky and radical deformation temperature. At the sticky temperature about 15-20% of the material is molten and at the solid phase is about 70% of the matter. This temperature range is the most harmful due to stickiness and massive deposit accumulation (Tran, 1997b).

4. EXPERIMENTAL

A high-temperature reactor to study the gas–particle equilibrium has been built in this thesis, and it has been exploited to investigate the gas–particle conversion in the conditions that can be found in a recovery boiler. Therefore, the amount of reactants try to mimic the elemental composition of the black liquor. The following chapter will clarify the phases of Figure 4.1. Figure 4.1 shows the main parts required to build a high-temperature test reactor. These parts are reactant feed, high temperature chambers, dilution, and particle measurement.

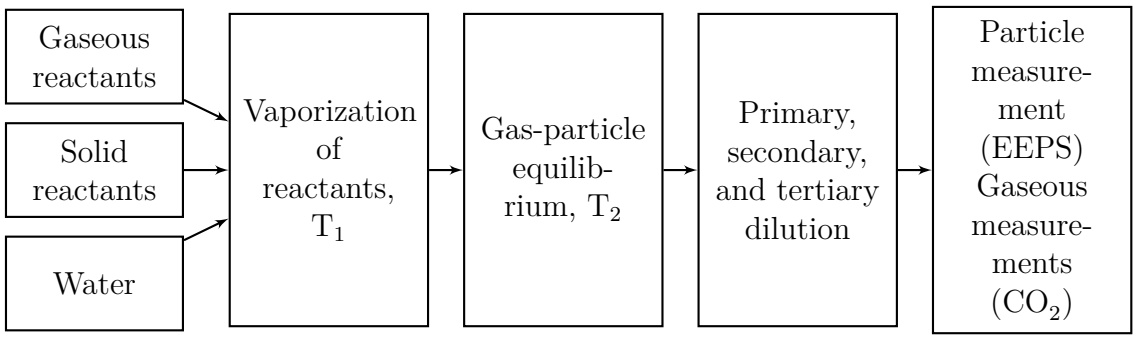

Figure 4.1: A flow chart of the measurement setup to measure gas–particle conversion.

4.1 Measurement setup

Experimental procedure is guided by the experimental setup shown in Figure 4.2. The setup consists of measuring equipment and diluters (see section 4.5) as well as the gas feeds (see section 4.4), alkali injections (see section 4.2 and 4.3) and vaporization, and residence time chambers. The chambers, made out of quartz glass, consist of two parts, the vaporization chamber (length 1090 mm and Ø 50 mm, residence time of the gas at 1000 °C is 14 seconds) and the residence time chamber (length 1390 mm and Ø 70 mm, residence time of the gas is at 500 °C 61 seconds and at 1,000 °C 37 seconds), which are placed inside two tube furnaces (darker gray boxes in Figure 4.2). The first tube furnace (made in physics workshop at TUT) is heated up to 1,000 °C, and it is placed vertically. Temperature of the other furnace (manufactured by Carbolite), placed horizontally, is changed between

500-1,000 °C to simulate the temperature gradient inside a recovery boiler furnace.

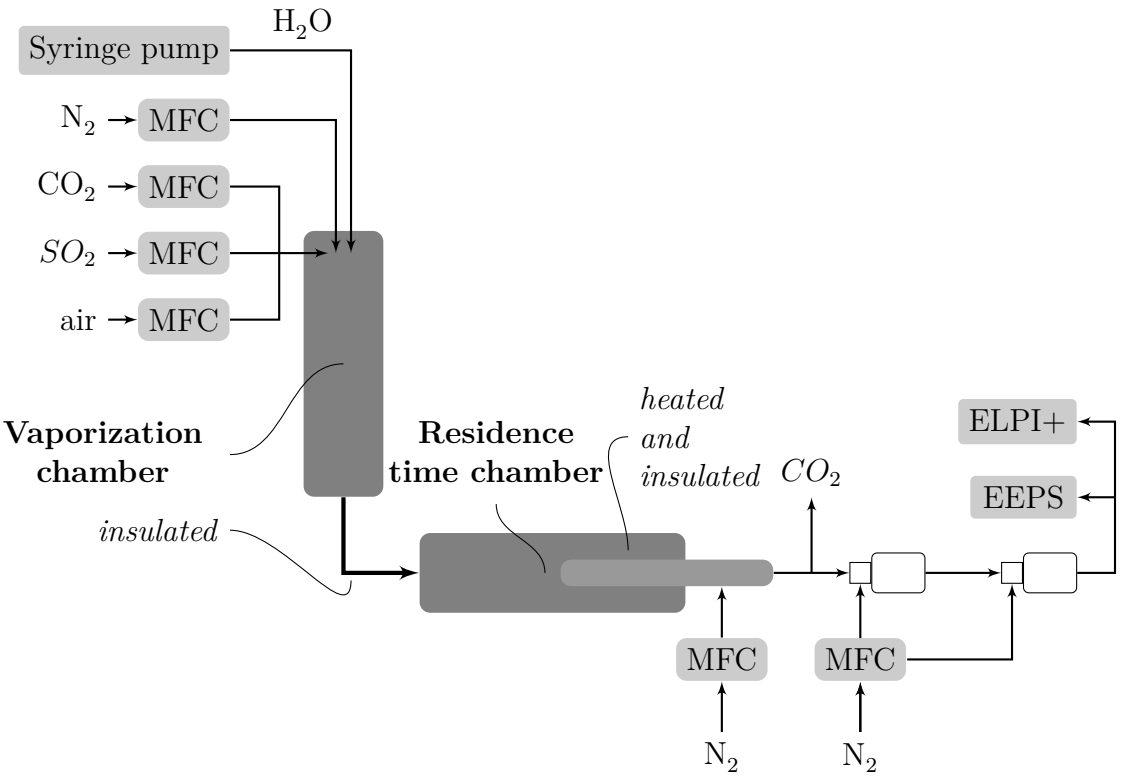

Figure 4.2: A detailed figure of the measurement setup to measure gas–particle conversion. Reactant feeding system is on the left (mass flow controllers, MFC and syringe pump) and on the right are diluters and measurement equipment.

The reaction chamber is insulated between the furnaces to maintain the heat in the system. The sample is taken using the hot diluter 40 cm inside from the outlet of the residence time chamber aiming to get a representative sample from high-temperature conditions. The reaction chamber is longer than the furnace 2, so additional heating and insulation over heater is used. An additional heater is adjusted to 500 °C. Aerosol sampling and dilution process is a two-step process, and it is described in detail in 4.5. For these measurements, ELPI+ (new model of ELPI) and EEPS were used. Measurement equipment operation principles are described in section 4.6. CO_2- analyzer was used with a sample flow of 1 slpm. The reactant feed system is described in 4.3, and the used reactant components are introduced in 4.2; also, used gas flows are described in 4.4.

Furnaces were heated (4 °C min^{-1}) to T_1=1,000 °C and T_2=500 °C, while heating all measurement equipment were tested and prepared to measure. Preparation included turning on the pumps and flows to the ejector diluters. When furnaces were at the right temperature the primary dilution ratio was tested, as explained

Table 4.1: Concentration range (in ppm) to use in the measurements.

	Concentration (ppm)				
Substance	Na	K	SO_2	Cl	total (mol-%)
low	2000	500	1000	50	0.35
high	3000	1000	2500	800	0.73

in section 4.5. Secondly, after adjusting the primary dilution ratio, the reactant feeding system, including the gas and water feed, and the mass flow controllers were switched on. ELPI+ was used as a monitoring equipment for the process, and stable ELPI+ currents indicated equilibrium in the system. Thirdly, the data from equilibrium situation was collected for some time, and after that, the primary dilution ratio was changed after reactant feed was turned off and replaced by 100% CO_2 flow to adjust dilution ratio.

The measurement cycle repeated the three steps described above. After two different primary DRs were measured, the T_2 could be raised. The measurements were made so that the furnace temperature T_2 was raised from 500 °C to 1,000 °C stepwise 250 °C at a time. The other option for temperature adjustments would have been to raise T_2 to 1,000 °C at first and then, stepwise lower the temperature towards 500 °C. Either way, the equilibrium between the gases and the particle formation is reached.

4.2 Sodium, potassium, and chloride feed rate

Sodium, potassium, and chloride injection rates have to be controlled and known because the experiment is used to define the impact of each compound or element to the gas-to-particle conversion. Guidelines for concentrations to use were gotten from the Metso database (4.1). Table 4.2 lists the values from the reactant solutions. Guideline values are the average values of elemental analysis of black liquor that have been corrected with release factors (calculated in Mikkanen (2000)) to flue gas. Guideline values can be used in selecting the reactant concentration combinations for reactant solutions.

There is no commercial equipment for measuring concentrations of sodium, potassium, and chloride from gas phase. Therefore, indirect method to control the amounts of reactants was used. A syringe pump manufactured by Cole Parmer and a glass pipette sprayer was used to spray the reactant solution into the vaporization chamber. The control to the amounts of reactants is based on the solution used. Different reactants solutions were to be made for each reactant combination listed in Table 4.2. The syringe pump was used with 50 ml syringe (diameter 26 mm) with a pumping speed of 24 ml per hour. The concentration of the reactant

Table 4.2: Concentrations (in ppm min^{-1}) of the solutions used in the measurements.

	Concentration (ppm min^{-1})				
Substance	Na	K	SO_2	Cl	total (mol-%)
w_{NaOH}	2500	0	0	0	0.25
w_{NaOH,SO_2}	2500	0	1500	0	0.40
$w_{NaOH,SO_2,KCl}$	2500	751	1500	425	0.52

solution was calculated based on the pumping feed of the solution.

The reactant solutions were made so that the NaOH and KOH were weighted based on calculations on the amount of the substance of 2 l min^{-1} air in the reaction chamber and the average concentrations from the values given in Table 4.1. The volume of the solution was 1,000 ml, and the weighted amount of NaOH and KOH were used to calculate the real amount of the substance and the concentration of the reactant solution. The real concentration of the solution was then used to calculate the real amount of NaOH and KOH, which were fed to the reaction chamber at the volume flow of 0.4 ml min^{-1} dissolved in deionized water. The quotient is calculated from the calculated amount of substance to the total amount of substance. Table 4.2 shows the injection rates of the Na^+ and K^+, sulphur dioxide, and chloride in each temperature and reactant combination.

4.3 Water feed

The water solution was fed to the vaporization chamber using a pipette sprayer. The pipette sprayer structure reminds the DeVilbiss model 40 nebulizer in Khan et al. (1990). The nebulizer in Khan et al. (1990) is a glass bulb full of liquid and a nozzle system. One nozzle is used to accelerate the gas flow, and the other is used to draw the liquid from the liquid reservoir. The spray is directed onto an impactor surface where the large particles are deposited and drained back to the liquid reservoir. The pipette sprayer has one crucial advantage compared to Khan et al. (1990); the liquid reservoir is isolated, and all of the formed particle are led to the aerosol. Both of these previously mentioned qualities enable continuous, stable, and specific concentration feed.

A pipette sprayer was bent from two glass pipettes. The tip of the other pipette was sanded to an oval shape, and it was bent so that the oval surface is perpendicular to the nitrogen flow through the other pipette. The tip of the nitrogen flow pipette was downsized to accelerate the nitrogen flow 0.35 slpm. Pipettes were placed between each other with a rubber band and the tips were positioned with a silicone rubber seal. Water was fed through the oval tip and a droplet formed on the tip. The accelerated nitrogen flow then ripped the droplet into a smaller droplets. With

this kind of sprayer, only a really small amount of salt is crystallized to the sprayer tip and the spray can be made continuous and stable.

In addition to the system described above, three other feeding systems were tested. The first was a pneumatic atomizer manufactured by TOPAS. It uses energy from compressed air to break up the liquid stream to the smallest droplets.

The second candidate for the water feeding system was an injection needle with syringe pump. The syringe pump was used to fed the water through a thin injection needle to the vaporization chamber. The needle system produced too-large droplets, and they did not evaporate in the vaporization chamber. Different size needles were used, but the surface tension of the water was the crucial factor for droplet size.

The third candidate was a vibrating orifice aerosol generator with syringe pump (Lechler GmbH Co). The vibrating orifice aerosol generator forms a thin filament of liquid by pumping the liquid through a small orifice (5-50 μm) with a syringe pump. The orifice is oscillated along its axis by means of piezoelectric crystal. With a constant liquid flow and a constant oscillation frequency, the generated aerosol distribution is monodisperse. The initial droplet diameter is 15-100 μm (Hinds, 1999). The problem with the vibrating orifice aerosol generator was that the salt crystallized into the nozzle of the generator. Therefore, the amount of reactants was unknown in the vaporization chamber.

4.4 Gas feeds

The gases used in these measurements were H_2O, CO_2, N_2, and O_2. Table 4.3 lists the gas flows and concentrations, which were kept constant during all of the measurements. Total flow rate in the reaction chamber was decided to be 2 l min^{-1}. For the calculations, the presented molar percentages indicate the same volume percentage of the total flow. Oxygen, carbon dioxide, and nitrogen were fed to the reaction chamber through Alicat mass flow controllers. The mass flow controllers control the flow by standard litres per minute. Controlling the flow with standard litres makes the calculations easier because of the standard conditions. Standard conditions in the flow control remove the need to take the gas temperature into account.

Oxygen was gained from the pressurized air (0.8 slpm), the nitrogen (0.63 slpm), and carbon dioxide (0.03 slpm) gained from the pressurized air were taken into account when calculating the amount of additional nitrogen and carbon dioxide. Additional nitrogen was also coming from the sulphur dioxide feed, and it was also taken into account in the gas feed calculations. Sulphur dioxide flow was 0.1 slpm, in which the portion of nitrogen is 0.097 slpm. There was a need for additional nitrogen (0.35 slpm) and carbon dioxide (0.2 slpm), which were gained from gas bottles. The total amount of gaseous feed was 3.980 slpm when the sulphur dioxide

Table 4.3: The concentrations of constant gas feeds and the standard flow rates of each gas taken from the gas bottle or line in the vaporization chamber. The constant gas feeds compose 99.1% of all feeds. Water was injected in liquid form with sodium, potassium and chloride. The volume flow of water was 0.4 ml min^{-1} which was approximately 0.498 dm^3 min^{-1} in gaseous form by assuming ideal gas.

Gas	Concentration (mol-%)	Flow (l min^{-1})
O_2	8.4	0.17
CO_2	11.7	0.23
H_2O	25.0	0.50
N_2	54.0	1.08
total	99.1	1.98

was taken into account.

4.5 Dilution methods

In this measurement setup, two different diluter were used. The first diluter (hot diluter) was placed inside the second furnace in the reaction chamber. The dilution ratio (DR, quotient between total flow and sample flow) of the hot diluter could be varied between 12-80. The nitrogen was preheated before the diluter to 500 °C, and it was heated in the diluter before mixing in the sample flow. Secondary and tertiary diluters were ejector diluters. They were used with a mass flow controller adjusted to 80 l min^{-1} flow through critical orifices to the ejector. The use of critical orifices assures that the dilution process was similar in both diluters. Between primary and secondary dilution, there was a CO_2-analyzer to monitor the primary dilution ratio while adjusting it with 100% CO_2.

The primary dilution ratio was determined with a 2 slpm 100% CO_2 gas feed to the reaction chamber at the temperature where measurement was planned to be performed. Mass flow controller was used to control the nitrogen flow to the diluter. T_2, the temperature of the reaction chamber, had an effect on the volume flow in the diluter and, therefore, the dilution ratio needed to be checked at each T_2.

The hot diluter was used to dilute the sample flow so that the vapour phase would nucleate in the dilution to a different mode than the particles formed in the residence time chamber by gas to particle conversion.

4.6 Particle monitors

An electrical low pressure impactor (ELPI, Dekati Oy) was used to measure particle number concentration as a function of the aerodynamic particle diameter. The ELPI uses a low-pressure impactor, which is a cascade impactor. ELPI employs electrical detection and provides near real-time information on the number-weighted

aerodynamic size distribution of aerosols. The aerodynamic diameter is useful in describing the behavior of particles in devices such as filters and impactors where inertial behavior dominates. In the ELPI, the aerosol particles are charged with corona charger before entering a low-pressure cascade impactor. Electrometers are used to measure the electric current produced by the electric charge carried by the impacted particles onto electrically isolated collection stages. ELPI can be used for real-time measurements with a high-time resolution 1 Hz (Keskinen et al., 1992). More details about ELPI are found in Table 4.4.

Engine Exhaust Particle Sizer, EEPS, by TSI exploits electrical detection of particles, according to an electrical mobility diameter. In the EEPS, the particles first pass through a negative corona diffusion charger and then a positive corona diffusion charger. The negative charger neutralizes the particles carrying a large positive charge. The particles are then introduced into a cylindrical classifier region at a radial location close to the inner cylinder. Particles with different electrical mobilities follow different trajectories in the electrical classifier. The particles are collected on a series of collection rings that are connected to an array of electrometers. Classification voltages are maintained in the three sections along the classifiers' length to extend the range of particle mobilities collected. Size distributions are calculated considering the electrometer signal, transfer functions, and the image charge effect on the electrometers (Dhaniyala et al., 2011). More details about EEPS are found in Table 4.4.

Table 4.4: A comparision of the EEPS and ELPI. Size range of an EEPS are electrical mobility diameters, and ELPI is an aerodynamic diameter. Electrometer array (EMA). ELPI used in these measurements was equipped with the filter stage (Marjamäki, 2003) and additional stage (Yli-Ojanperä et al., 2010), so the particle size range covered 6-10,000 nm. (Dhaniyala et al., 2011)

Characteristics	EEPS	ELPI
Size range (nm) 0	5.6-560	6-10,000
Measurement time (s)	1	1
Particle detector	EMA	EMA
Size channels per decade	16	14
Typical aerosol flow rate (dm^3 min^{-1})	10	10
Typical sheat air flow rate (dm^3 min^{-1})	40	none

4.7 Safety assessment

Working in the laboratory requires knowledge about chemicals and safety. It is crucial to know chemicals and gases used in the reaction furnace as well as, their reactivity with other chemicals, including water. It is also necessary to know what

kind of exhaust gases are emitted, so that the after-treatment is sufficient, and any harmful gases are not released in the laboratory. All the information can be found in a safety data sheet. Appendix tables 1 and 3 list the reactants used in these measurements. There is another appendix table (2) for a chemical compound that could be formed in the reaction chamber.

In this study, hydrochloric acid, sodium, and potassium hydroxides are not concentrated. Acid and bases are diluted so that the needed concentrations are achieved in the reaction chamber. In the reaction chamber, a gaseous compound might form sodium sulphate, sodium carbonate, potassium sulphate, and potassium carbonate, which are not toxic to humans or the environment.

In addition to chemicals, the study uses gases as reactants. Gases are stored in high-pressure gas bottles so theirs usage and storing must be planned carefully. Gas bottles should be stored in fume hood. When in use, the bottles are kept in a distance from the hot furnaces.

Two furnaces used in this measurements are kept at high temperatures at 500-1,000 °C. The first furnace is constantly kept at 1,000 °Celsius. Therefore, it is necessary to be aware of the hot surfaces and hot gas flows. The hot surfaces emit particles, which need to be filtered or removed from the room because of the possible health risks. The particles formed in the reaction chamber are exhausted from the measuring equipment outlets. Thus, those particles need to be filtered.

5. RESULTS

5.1 Lognormal fit for particle size distribution

Particle size distributions taken to more detailed analysis were measured with an EEPS. A few examples of particle size distributions can be found in Figures 5.1 and 5.2. Lognormal fit was made as a three mode fit (example in Figure 5.2a) except for four individual particle size distributions (example in Figure 5.2b) for which the lognormal distribution fit was made differently because the distribution consisted only of two modes. There was no difference in the behavior of the second mode compared to the first mode. For further analysis, the first and the second mode were combined when the number and volume concentrations were considered. If the particle size distribution consisted of two modes, the second mode is compared with the third mode. Lognormal fit needed starting values: the number of modes, the highest point of distribution, and the width of the particle mode. Starting values were estimated from a log–log -figures of the measured particle size distributions. Those values were used to calculate the best fits for the measured particle size distribution. The lognormal fit code is based on unconstrained nonlinear optimization by *fminsearch*-function of Matlab. The code basically minimizes the error between the sum of the fits and the measured particle size distribution.

Comparison between EEPS and ELPI+ measurements were made $w_{NaOH,SO_2,KCl}$-feed (see Table 4.2) with a primary dilution ratio of 80. The temperature of the residence time chamber was 750 °C. Data can be seen in Figure 5.3. EEPS and ELPI+ have measured a similar shape particle size distribution. There is a difference between the mean particle diameters in EEPS and ELPI+ particle size distributions, especially in particle mode 3. The difference at the third mode is likely caused by an effective density of the particles. By a rough analysis of the effective density of particle at the mode 3 can be made based on the mean diameters of the particle size distributions. Estimated mean diameters for calculations were D_p=121 nm (from Table 5.3) and D_a=200 nm (estimated from Figure 5.3). These diameters indicate that the effective density on the particle is 2.7 g cm^{-3} which nearly corresponds to the density of different inorganic salts (see Table 3.2).

Tables 5.1, 5.2, and 5.3 show characteristic values obtained from the lognormal fit. Values noted with the symbol * are not comparable values because those are outside of the EEPS measurement range. Three different primary dilution ratios were used

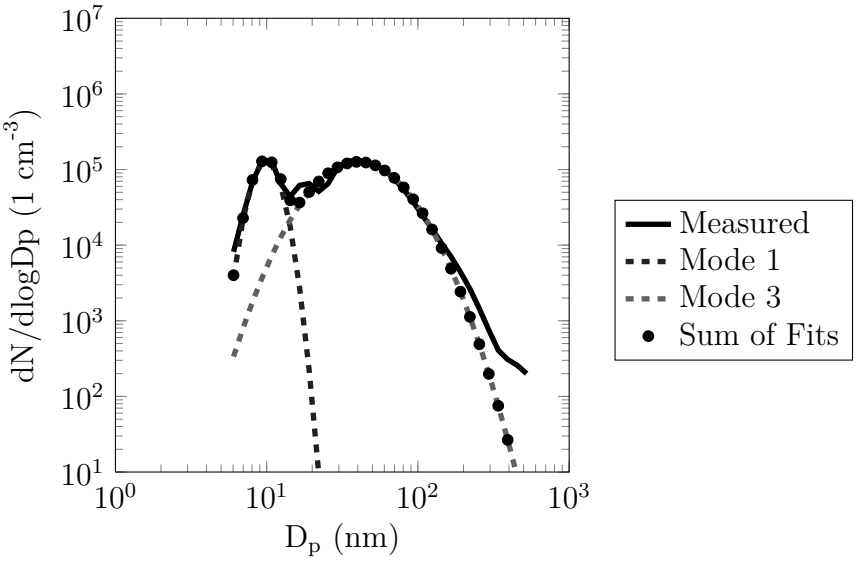

a T_2=500 °C, primary DR 12

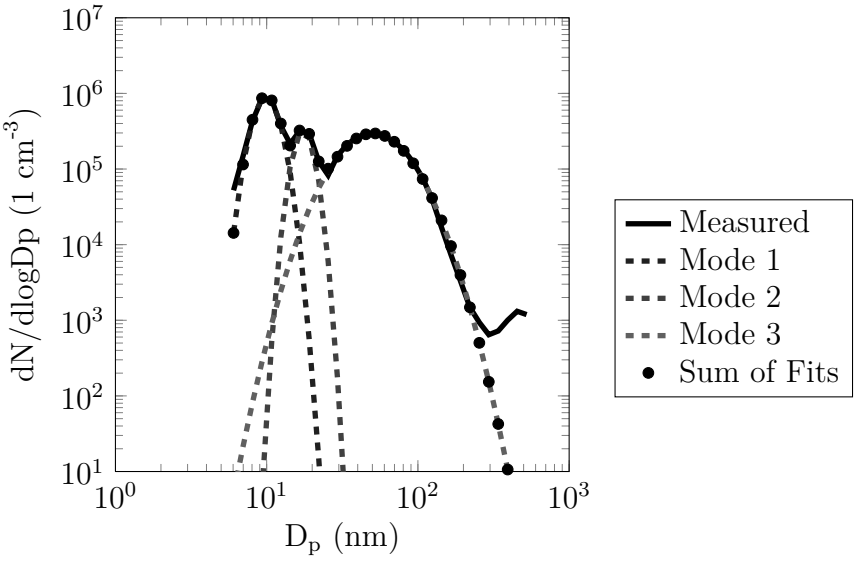

b T_2=500 °C, primary DR 80

Figure 5.1: Particle size distributions measured with EEPS and lognormal fits.w_{NaOH}-feed was used. Primary DR had an effect on width of the larger mode. Higher primary DR has a narrower larger mode, and the height of the first mode increases. T_2 is the adjusted temperature of residence time chamber.

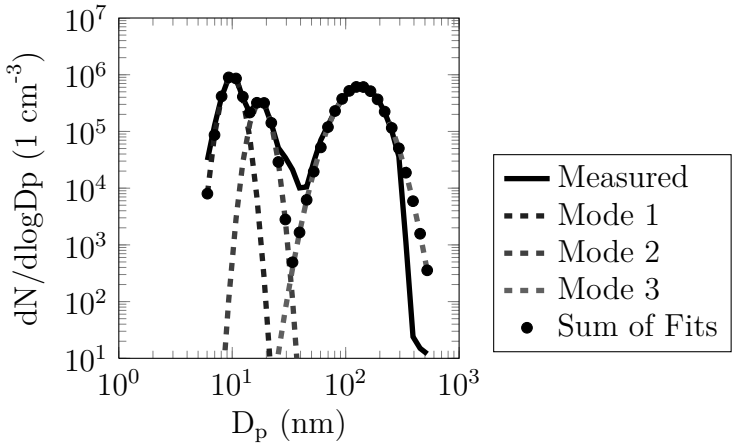

a T_2=500 °C

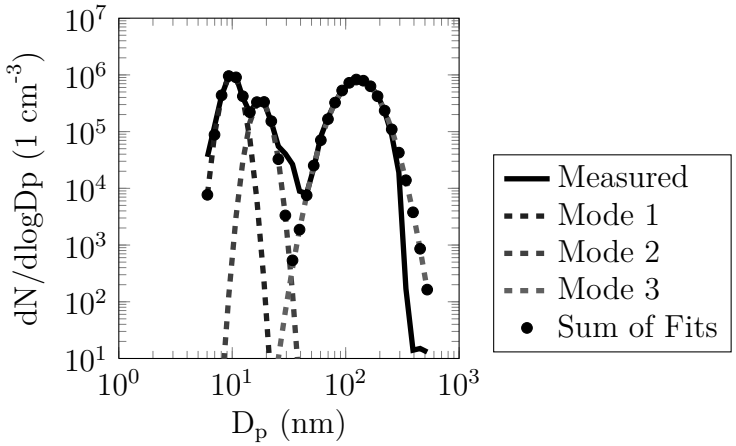

b T_2=750 °C

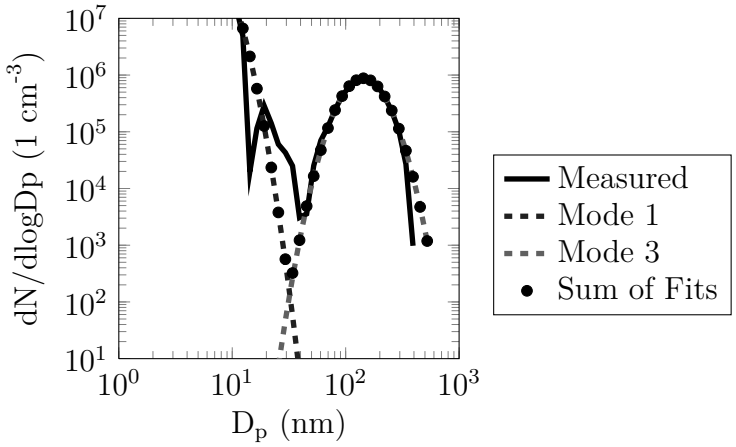

c T_2=1,000 °C

Figure 5.2: Particle size distributions measured with EEPS and lognormal fits. The results shown here were measured with $w_{NaOH,SO_2,KCl}$-feed and primary DR 80. The higher the temperature, the smaller the number concentration of the largest mode becomes and the bigger the number concentration of the first mode. T_2 is the adjusted temperature of residence time chamber.

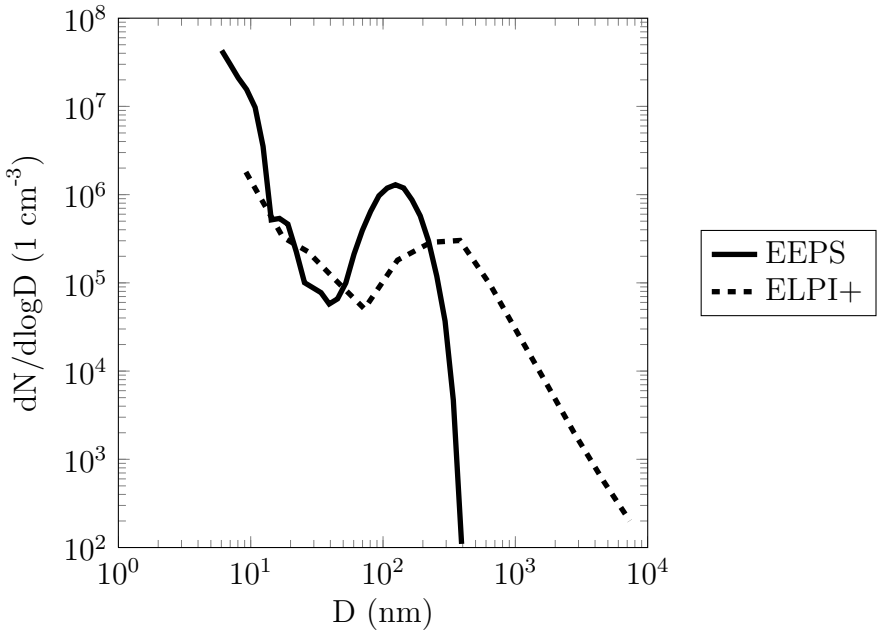

Figure 5.3: Particle size distributions measured with EEPS and ELPI+ with $w_{NaOH,SO_2,KCl}$-feed 750 °C with a primary dilution ratio of 80. EEPS and ELPI+ particle diameters were different from each other: EEPS diameter is electrical mobility diameter and ELPI+ diameter is aerodynamic diameter.

when measuring the simplest reactant feed combination (see results in Table 5.1): air 0.8 slpm, 0.35 slpm N_2, and w_{NaOH}-feed. At 500 °C, none of the modes differed from each other when changing the primary dilution ratio. At T_2=750 °C, there was a slight difference between the primary dilution ratio of 12 and DR of 36. It also seems that the measurement with a primary DR of 80 produces similar particle size distribution, like the measurement when the primary DR was 36. At T_2=1,000 °C, the primary dilution ratio had considerable effect on the particle mean diameter. The particle mean diameter decreased while the primary DR raised. The results indicate that the higher primary DR is useful to shift the nucleation mode to the smaller mean diameter while the third mode does not change.

Reactants were changed to study the effect of different compounds in the particle formation. Results from measurement with different reactants are shown in Tables 5.2 and 5.3. Results are given for two different primary dilution ratios in three different T_2 furnace temperatures.

5.2 Background concentration

Background concentration measurements were made with ELPI+ at T_1 =1,000 °C and T_2 =1,000 °C with 1.1 slpm air, deionized water 24 ml h^{-1}, and 0.35 slpm of

Table 5.1: Characteristic values for lognormal distributions from measurement results with reactants feeds: air 0.8 slpm, 0.35 slpm N_2, and w_{NaOH}-feed.

		500 °C			750 °C			1,000 °C		
		DR 12	DR 36	DR 80	DR 12	DR 36	DR 80	DR 12	DR 36	DR 80
Mode 1	D_{mean} (nm)	9.89	9.97	9.89	5.95	10.1	9.94	11.6	9.63	7.43
	std	1.20	1.19	1.19	1.39	1.17	1.19	1.36	1.26	1.37
	N (1 cm^{-3})	7.76 $\cdot 10^4$	$2.62 \cdot 10^5$	$5.04 \cdot 10^5$	$7.81 \cdot 10^6$	$4.75 \cdot 10^5$	$7.23 \cdot 10^5$	$2.44 \cdot 10^8$	$3.11 \cdot 10^8$	$1.48 \cdot 10^8$
Mode 2	D_{mean} (nm)		17.2	17.5		16.9	17.5			
	std		1.14	1.14		1.19	1.15			
	N (1 cm^{-3})		$1.62 \cdot 10^5$	$3.30 \cdot 10^5$		$3.83 \cdot 10^5$	$4.96 \cdot 10^5$			
Mode 3	D_{mean} (nm)	40.5	49.4	50.5	51.7	42.1	41.3	75.6	57.3	49.5
	std	1.74	1.57	1.57	1.50	1.68	1.62	1.23	1.26	1.30
	N (1 cm^{-3})	$9.69 \cdot 10^5$	$1.74 \cdot 10^6$	$2.09 \cdot 10^6$	$1.95 \cdot 10^6$	$1.87 \cdot 10^6$	$1.71 \cdot 10^6$	$9.29 \cdot 10^5$	$1.47 \cdot 10^6$	$8.54 \cdot 10^5$

Table 5.2: Characteristic values for lognormal distributions from measurement results with reactants feeds: air 0.8 slpm, 0.35 slpm N_2, and w_{NaOH,SO_2}-feed.

		500 °C		750 °C		1,000 °C	
		DR 12	DR 80	DR 12	DR 80	DR 12	DR 80
Mode 1	D_{mean} (nm)	9.85	9.95	9.87	9.93	9.57	5.08*
	std	1.18	1.17	1.17	1.17	1.27	1.42
	N (1 cm^{-3})	$7.60{\cdot}10^4$	$5.08{\cdot}10^5$	$7.88{\cdot}10^4$	$5.31{\cdot}10^5$	$1.77{\cdot}10^7$	$2.00{\cdot}10^7$
Mode 2	D_{mean} (nm)	18.4	17.8	18.4	17.8		
	std	1.21	1.17	1.22	1.18		
	N (1 cm^{-3})	$8.15{\cdot}10^4$	$4.35{\cdot}10^5$	$8.78{\cdot}10^4$	$4.55{\cdot}10^5$		
Mode 3	D_{mean} (nm)	134	133	125	129	140	143
	std	1.40	1.43	1.39	1.40	1.42	1.43
	N (1 cm^{-3})	$5.96{\cdot}10^6$	$5.04{\cdot}10^6$	$6.29{\cdot}10^6$	$6.40{\cdot}10^6$	$6.40{\cdot}10^6$	$7.34{\cdot}10^6$

Table 5.3: Characteristic values for lognormal distributions from measurement results with reactants feeds: air 0.8 slpm, 0.35 slpm N_2, and $w_{NaOH,SO_2,KCl}$-feed and 0.2 slpm of gaseous CO_2.

		500 °C		750 °C		1,000 °C	
		DR 12	DR 80	DR 12	DR 80	DR 12	DR 80
Mode 1	D_{mean} (nm)	9.83	9.87	4.49*	3.51*	7.64	9.40
	std	1.19	1.18	1.73	1.72	1.40	1.32
	N (1 cm^{-3})	$6.13{\cdot}10^4$	$4.46{\cdot}10^5$	$4.03{\cdot}10^5$	$9.13{\cdot}10^6$	$1.03{\cdot}10^7$	$5.82{\cdot}10^8$
Mode 2	D_{mean} (nm)	18.5	18.1				
	std	1.20	1.20				
	N (1 cm^{-3})	$6.00{\cdot}10^4$	$4.25{\cdot}10^5$				
Mode 3	D_{mean} (nm)	127	121	129	121	127	129
	std	1.41	1.43	1.39	1.42	1.40	1.42
	N (1 cm^{-3})	$5.62{\cdot}10^6$	$5.78{\cdot}10^6$	$8.04{\cdot}10^6$	$1.01{\cdot}10^7$	$7.59{\cdot}10^6$	$6.95{\cdot}10^6$

nitrogen with primary DRs 19.2 and 50. Total concentrations were calculated from ELPI+ data by assuming unit density for studied particles. The diameter ranges are not the same for EEPS and ELPI+. Therefore, ELPI+ results were calculated from a diameter range of 6-490 nm to have more comparable results with EEPS. Total number concentration for DR 19.2 was $2.01 \cdot 10^7$ cm^{-3} and for DR 50 $1.96 \cdot 10^7$ cm^{-3}. These results are slightly comparable with w_{NaOH}-feed (T_1 =1,000 °C and T_2 =1,000 °C) with DR 12 and DR 80. It is notable that ELPI+ results are underestimating the number of larger particles; however, the amount of larger particles is smaller and does not have significant effect on the total number concentration. The background concentrations were measured with a lower primary DR than that was used afterwards. Lower primary DR might raise the total particle number concentration and enable the growth of the particle mean diameter. Background concentrations (with DRs 19.2 and 50) compared to the DR80 results indicate that the changes in particle size distributions with different reactant feeds were detectable by comparing the particle size distributions.

5.3 Particle number and volume concentrations

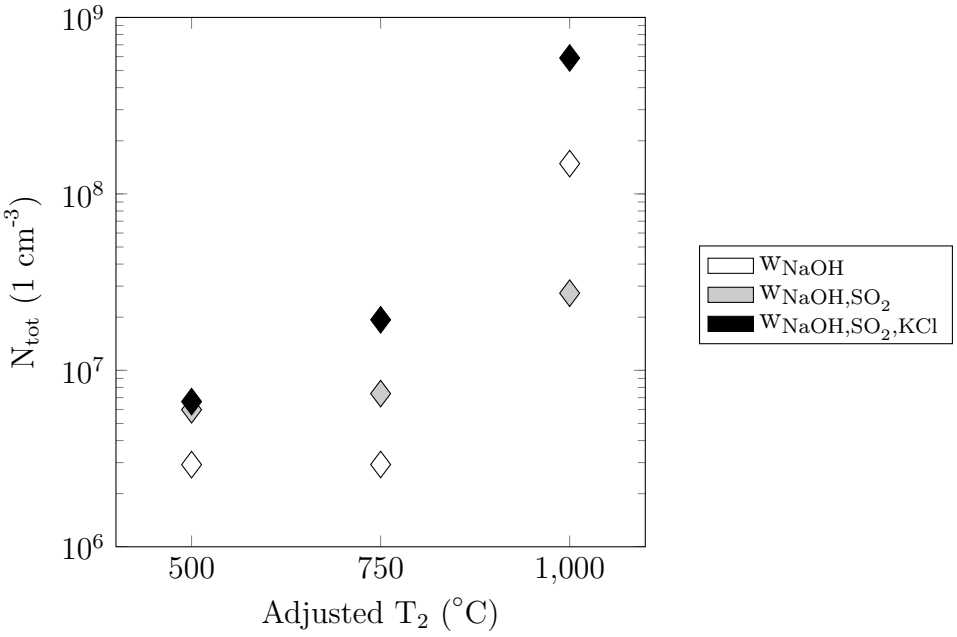

Figure 5.4: Total number concentrations of diluted sample with different reactant feeds.

In Figure 5.4, the total number concentrations are shown for different reactant feeds. The feeds are chosen so that the effect of each reactant addition should be notable. This is the case when comparing w_{NaOH}- and $w_{NaOH,SO_2,KCl}$-feeds with each

other in Figure 5.4. Total number concentration is decreased due to efficient particle formation caused by lowered temperature. When comparing Figures 5.4 and 5.5, it can be noticed that with w_{NaOH}-feed the total number concentration of particles was decreased when the adjusted temperature (T_2) was lowered from 1,000 °C to 500 °C. At the same time, the total volume concentration of particles increased. This phenomena can partly be explained by the decrease of gaseous reactants in the gas phase when the T_2 was decreased. Also, the wall losses caused by lower temperatures at the residence time chamber can affect the results. At 750 °C, there were more gaseous compounds in the residence time chamber than at 500 °C. The amount of gaseous compounds can be estimated based on particle volume concentration.

Total volume concentration of particles with w_{NaOH,SO_2} and $w_{NaOH,SO_2,KCl}$-feeds were nearly constant. The only difference in the total volume concentration was observed when the T_2 decreased from 750 °C to 500 °C. The similarity of the total volume concentration curves refers to sulphation of SO_2. Sulphate acts as a particle-forming agent at temperatures below 1,000 °C. This can also be seen in the results in Table 5.1 and 5.2, the latter of which is one with an SO_2 addition. The SO_2 addition had a minimal effect on the mode 1, but the mode 3 mean diameter grew from 40-75 nm to 125-143 nm. This growth can be caused by reactions between alkali metals and SO_2. The possible reaction mechanisms are shown in reaction equations 3.8 and 3.3 or 3.10 and 3.11. The latter one is the most uncertain. The high temperature (over 1,300 °C) is needed for reactions 3.10 and 3.11 to happen (Mikkanen et al., 1999).

Mode particle number and volume concentrations were calculated from lognormal fit data for each mode separately. The results for mode 1 and mode 2 were combined to mode 1&2. Combined mode 1&2 gave a possibility to compare bi-modal and originally tri-modal size distributions by characteristic values.

Figures 5.7 and 5.8 show the number concentrations of each mode of the particle distributions. Mode 1 has an decreasing trend in number concentration as a function of decreasing temperature for each reactant feed and temperature. Decrease in number and volume concentration in mode 1 is a function of lowered temperature. This can be treated as an indicator for particle formation processes. There are more small particles (mode 1) at 1,000 °C than at below 750 °C.

At T_2 1,000 °C, the volume concentration of mode 3 (in Figure 5.6) w_{NaOH}-feed is nearly the same or a little less than at below T_2=750 °C. The number concentration of mode 3 at 1,000 °C in Figure 5.7 is decreased compared to 750 °C. At 500 °C, or when the vapour is cooled down from 1,000 °C to 500 °C thermophoresis, wall losses and the efficient particle formation lower the concentration of vapours. The lower concentration of vapours can also be seen in the mode 1&2 particle number and volume concentration, which is the lowest at 500 °C.

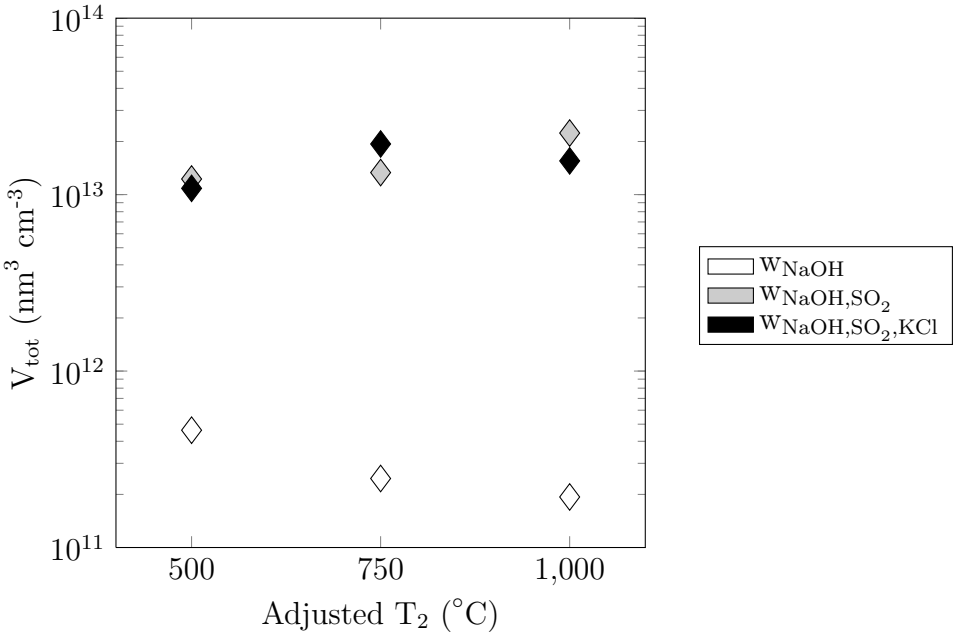

Figure 5.5: Total volume concentrations of diluted sample with different reactant feeds.

Figure 5.6 shows the mode volume concentrations with two different reactant feeds w_{NaOH} and w_{NaOH,SO_2}, with the difference of SO_2 present. A possible explanation for the decrease in total volume concentration is the oxidation of SO_2 to sulphate, which lowers the concentration of vapours. Alkali sulphates are stable in temperatures below 1,000 °C and, therefore, the mode 3 volume concentration does not change much as a function of lowered temperature. Cases with and without SO_2 gas (Figure 5.6) are the most interesting in terms of volume concentration of mode 3 because the trends are different from each other as a function of decreasing temperature. This trend can be explained by different chemical reactions in the gas phase, thermophoresis, and wall losses. It is notable that CO_2 (gained from air) is a limiting agent of the oxidation of carbon dioxide; in the case of a surplus of CO_2, mode 3 volume concentration might be higher.

In Figure 5.7 the effect of SO_2 on particle formation in terms of number concentration is shown. The figure can be compared to Figure 5.6. In the case of w_{NaOH}-feed, the mode 1 particle volume concentration might be formed via reaction 3.10 in the dilution. Part of the alkali vapours might condense to hydroxide compounds. The formation rate of carbonate and hydroxide particles can be high during the dilution when the hot vapours are cooled down. Reactant feed, w_{NaOH,SO_2}, is nearly the same as w_{NaOH} in the case of CO_2 and OH^-, but in Figure 5.7 the difference in mode 1 particle number concentration at 1,000 °C compared to that of 500 °C is remarkable. OH^- and oxidizing CO_2 are forming particles because of high concentrations of

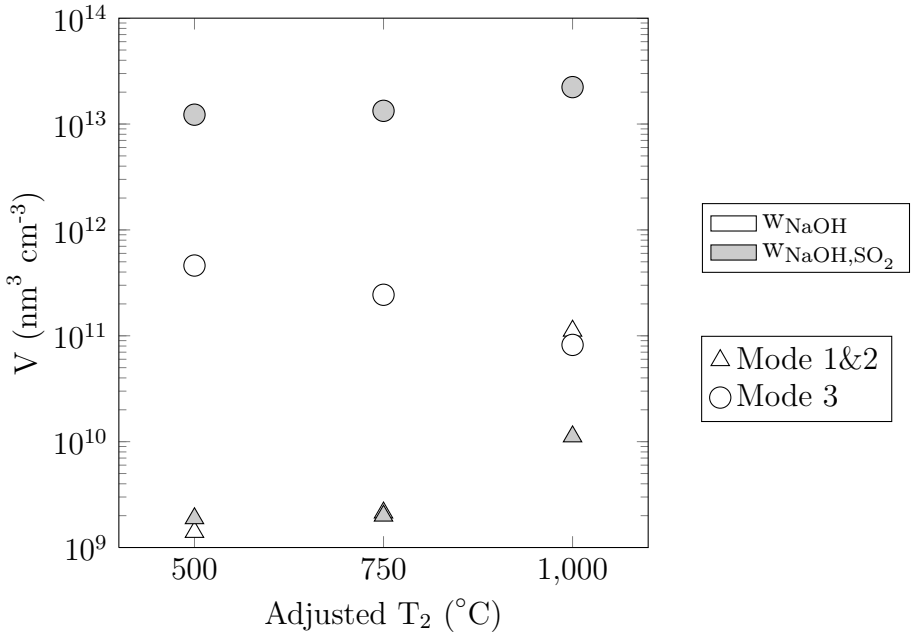

Figure 5.6: Volume concentrations of different modes with different reactant feeds. Reactant feeds have an effect on mode volume concentration.

vapours in the dilution. This means that in Figure 2.1, nucleation and condensation of CO_3^{2-} and OH^- from the vapour phase to particles is enhanced in the dilution. The number concentration of the mode 1 w_{NaOH,SO_2}-feed is higher at 1,000 °C than at 750 °C because of the nucleation in the dilution. This theory is supported by the fact that w_{NaOH}-feed mode 3 number concentration is increased when T_2 is lowered, whereas in the case of w_{NaOH,SO_2}-feed, the mode 3 particle number concentration is almost the same. The growth of mode 3 in the case of w_{NaOH} indicates that mode 3 consists of something that is condensing to particles when the temperature is lowered from 1,000 °C. Carbonates and hydroxides are good candidates for this kind of behaviour.

Comparing nucleation mode number concentrations in cases of w_{NaOH,SO_2}- and $w_{NaOH,SO_2,KCl}$-feed (in Figure 5.8), the difference in reactants is mainly Cl^- because K and Na should react equally. It is known that at a low temperature (500 °C), alkali chloride is in solid form. This means that alkali chloride is condensing on existing particle surfaces or nucleating (see Figure 2.1) at low temperatures. At 750 °C, less alkali chloride is in the gas phase and more liquid alkali chloride is on the particle surface. Mode 1 particle number concentration at 750 °C is higher when there is alkali chloride as one of the reactants. This might indicate that more gaseous compounds were present in the gas phase compared to the situation when there was no alkali chloride. At the same time, mode 3 number concentration

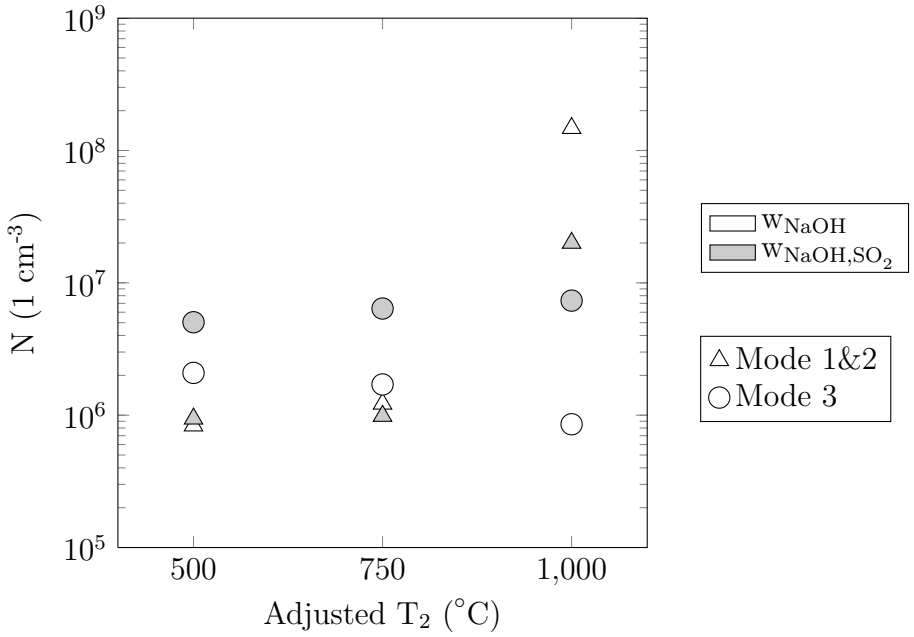

Figure 5.7: Mode number concentrations to show the effect of SO_2 gas addition for the particle formation. It is notable that CO_2 (gained from air) is limiting agent of the oxidation of carbon dioxide; in case of surplus of CO_2 mode 3 volume concentration would be higher.

($w_{NaOH,SO_2,KCl}$-feed) at 750 °C does not differ from the mode 3 w_{NaOH,SO_2}-feed.

Figure 5.9 presents the mode volume concentrations calculated from 5.8. Rough estimation of sodium chloride content in the mode 1 can be calculated from Figure 5.9 based on density ρ_{NaCl} = 2.17 g cm^{-3} and M_{NaCl} = 58.44 g mol^{-1}. For mode 3 density, $\rho_{Na_2SO_4}$ = 2.7 g cm^{-3}, and M_{NasSO_4} = 142.05 g mol^{-1} can be found by multiplying volume concentration with density (see equation 5.1).

$$\begin{aligned} \text{volume fraction (ppm)} &= \frac{\text{mass fraction (mg m}^{-3}) \cdot 24.1 \text{ dm}^3 \text{ mol}^{-1}}{M \text{ (g mol}^{-1})} \\ &= \frac{V \text{ (cm}^3 \text{ m}^{-3}) \cdot \rho \text{ (g cm}^{-3}) \cdot \ 24.1 \text{ dm}^3 \text{ mol}^{-1}}{M \text{ (g mol}^{-1})} \end{aligned} \quad (5.1)$$

The calculated volume fractions for NaCl are 7 ppb, 630 ppb, and 50 ppm, responding to temperatures of 500, 750, and 1,000 °C. Volume fractions of NaCl calculated from the change in mode 1 in Figure 5.9 show that more NaCl is in the gas phase to form mode 1 particles in the dilution. Volume fraction of 50 ppm at T_2=1,000 °C is a little over fifth of the volume fraction of Cl^- fed to the vaporization chamber. Part of the Cl^- has deposited on the walls, and part of it might be at larger particles.

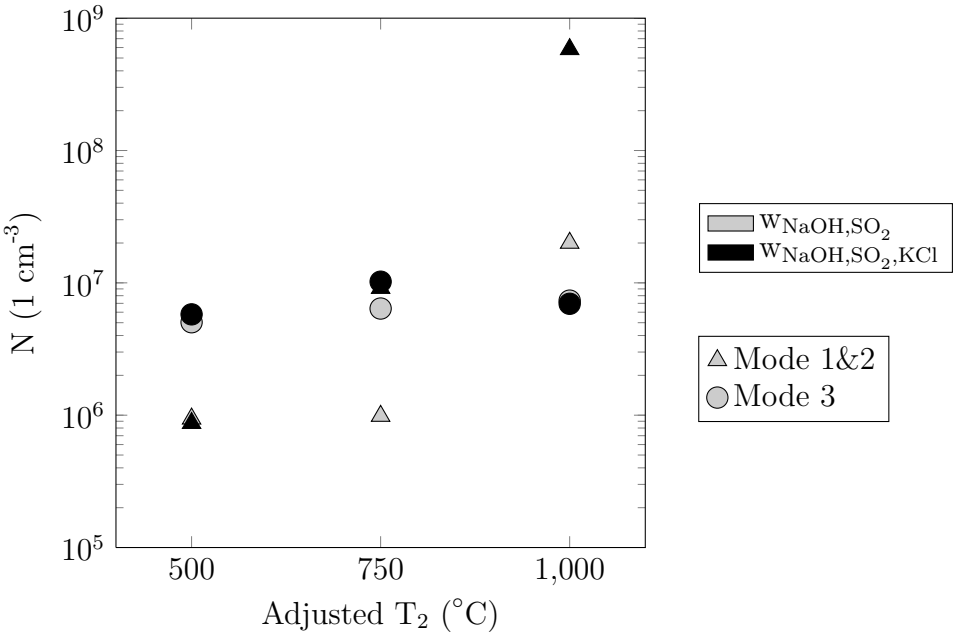

Figure 5.8: Number concentrations of different modes with different reactant feeds and the effect of Cl^- to the particle formation.

The calculated volume fractions of Na_2SO_4 ($w_{NaOH,SO_2,KCl}$-feed) are 500 ppm, 890 ppm, and 690 ppm responding to temperatures of 500, 750, and 1,000 °C. The oxidation of SO_2 is not restricted, but the formation of Na_2SO_4 is restricted by the amount of SO_2 because both Na^+ and K^+ (sum 3251 ppm against 1500 ppm of SO_2) can act as a compound-forming cation.

5.4 Future studies and improvements to the test reactor

The are number of error sources. One error source is the pipette sprayer, as there are some crystallization of the salts to the pipette surface. The biggest error source involves the deposition losses to the walls and especially the losses of the reactants to the cold glass wall. These deposition losses will decrease the amount of reactants fed in the vaporization chamber. The dilution process is a bit uncertain as a function of temperature; therefore, it is right to assume that there are some error sources–e.g., unwanted nucleation. Measurement equipment are not chosen optimally because EEPS underestimates the amount of large particles.

Based on the error analysis and lack of chemical information, there is a need to improve the test reactor. Major improvement should be made to the top of the vaporization chamber. The upper part of the chamber should be heated as hot as rest of the chamber, which will minimize the deposition losses of the reactants. Heating to the top part of the vaporization chamber might cause, for example, plugging of the

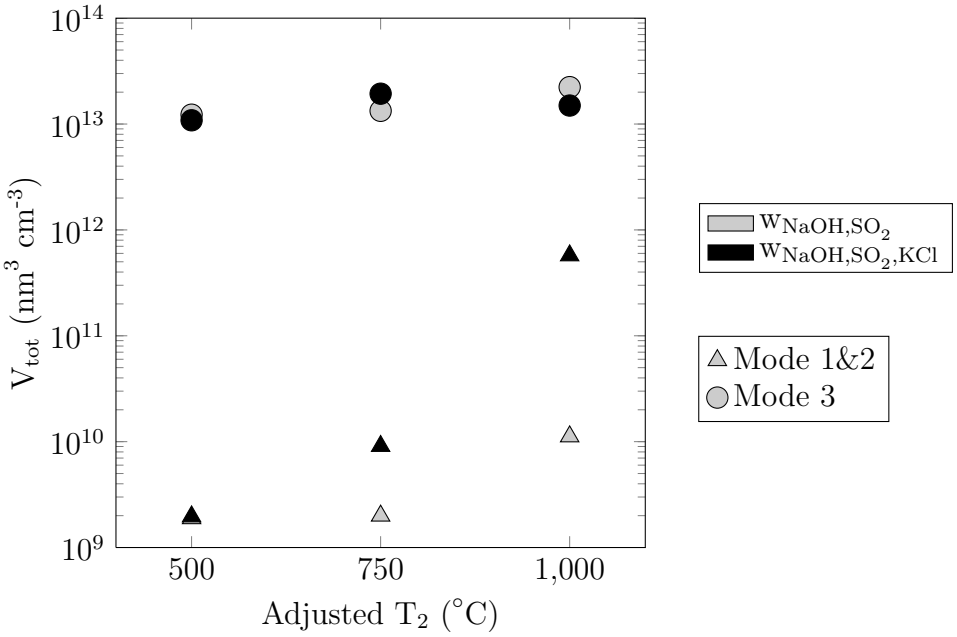

Figure 5.9: Volume concentrations of different modes with different reactant feeds and the effect of Cl^- to the particle formation.

pipette head. Plugging is easy to notice from the decreased particle concentrations or total current of ELPI. If possible, the pipette sprayer could be replaced with a new, better-known aerosol generator. Temperatures and temperature gradients should be measured, monitored and modeled. Possible cold spots should be noticed (measured or modeled) and attempted to be added to a heating element or insulation.

Dilution should be tested with a cold primary dilution to find out how the hot dilution affects the nucleation processes in the dilution. The cold primary dilution nucleates most of the vapours, and part of the vapour might be lost to walls by thermophoresis. With a cold primary dilution, the amount of gaseous species could be calculated from the nucleation mode, and these results could be compared to the hot primary dilution case. The difference gained from the calculations would indicate the amount of gaseous species went to mode 3 particles.

Chemical characterization from impactor collections should be done to have information about the composition of different diameter particles. This might also provide information about the nucleation processes and give insight about the reactivity of different compounds found in the reactor. Transmission electron microscopy samples should also be collected to find out the morphology of the particles. In order to apply this aerosol reaction chamber to corrosion and fouling tests, repeatability of the particle generation needs to be verified.

6. CONCLUSIONS

The objective of this thesis was to build an aerosol test reactor to study gas-to-particle conversion in a high temperature environment. The developed test reactor enables temperature and reactant concentration control. The test reactor consists of a reactant feeding system, a vaporization chamber, a residence time chamber, and dilution with particle measurement equipment. A reactant feeding system was developed in this thesis. It consists of a syringe pump and a pipette sprayer, which are used to generate droplets into a vaporization chamber. Water droplets where alkali metal salts were dissolved are carried in nitrogen to the vaporization chamber, where other gaseous reactants are added to the gas phase. Droplets are vaporized at 1,000 °C and then led to a residence time chamber to form a gas–particle equilibrium at a certain temperature between 500-1,000 °C.

The sample is taken inside the residence time chamber with a hot diluter. Primary dilution ratio can be varied, but the secondary and tertiary dilution ratios are constant because they are operated with room temperature nitrogen and ejector diluters. Reactant feeds for this thesis were selected from black liquor recovery process, where black liquor is combusted to be reused in paper pulping. When black liquor is combusted, different inorganic species are vaporized, and those vapours form particles via gas-to-particle conversion. Besides inorganic gases the black liquor combustion produces fly ash and carryover-particles of unburned black liquor. All of the previous ones are the main reasons for unscheduled shutdowns, fouling, and corrosion in Kraft recovery boilers.

In this thesis, a few different reactant feed combinations were tested, and a change in particle formation was seen. There were substantially fewer particles with w_{NaOH}-feed than with w_{NaOH,SO_2} gas. The SO_2 dominates the whole particle formation by forming alkali sulphates. If SO_2 is removed from the process, the formation of alkali carbonates in the dilution can be seen with w_{NaOH}-feed. This was observed by studying the formation of nucleation mode. With w_{NaOH}-feed, the nucleation mode particle number concentration was increased compared to the situation w_{NaOH,SO_2}-feed. There were indirect indications of the presence of alkali chlorides in the $w_{NaOH,SO_2,KCl}$-feed situation at the nucleation mode. The nucleation mode particle number concentration is decreased, while the larger mode is nearly stable when residence time chamber temperature is lowered from 1,000 °C to 500

°C. At 1,000-750 °C, the alkali sulphate particles should be stable, but the alkali chlorides should be in the vapour phase. Therefore, the presence of alkali chlorides is expected to be seen as a decrease in the concentration of the nucleation mode, when the temperature of the residence time chamber is lowered.

These results give an optimistic basis for further studies. The change in particle size distribution can been seen in the case of changing temperature or concentration. In the future, more tests should be performed, and the reliability of this aerosol reactor should be tested and an impactor collection for mass balance calculations should be made. The comparison between reaction chamber measurements and real Kraft recovery boiler measurement would be interesting.

This reactor has significant potential to study the chemical composition of the particles in different temperatures and with different reactant feeds. The results from these measurements can be added in a Computational Fluid Dynamics model. Some long-time exposures for different materials can be performed by varying the reactants and temperatures. The reaction chamber can also be used to study different kinds of inorganic species relative to the corrosion and fouling processes in power plants or elsewhere in the industry.

BIBLIOGRAPHY

Terry Adams. General characteristics of kraft black liquor recovery process. In Terry N. Adams, editor, *Kraft Recovery Boilers*. TAPPI Press, 1997.

John E. Brockmann. Aerosol transport in sampling lines and inlets. In Pramod Kulkarni, Paul A. Baron, and Klaus Willeke, editors, *Aerosol Measurement - Principles, Techniques, and Applications*. John Wiley & Sons, 3rd edition, 2011.

J. H. Cameron and Kristin Goerg-Wood. Role of thermophoresis in the deposition of fume particles resulting from the combustion of high inorganic containing fuels with reference to kraft black liquor. *Fuel Processing Technology*, (60):49–68, 1999.

Suresh Dhaniyala, Martin Fierz, Jorma Keskinen, and Marko Marjamäki. Instruments based on electrical detection of aerosols. In Pramod Kulkarni, Paul A. Baron, and Klaus Willeke, editors, *Aerosol Measurement -Principles, Techniques, and Applications*. John Wiley & Sons, 3rd edition, 2011.

Arkke J. Eskola, Jorma K. Jokiniemi, Kari E. J. Lehtinen, and Esa Vakkilainen. Modelling alkali salt deposition on kraft recovery boiler heat exchanges in the superheater section. *TAPPI*, 3, 1998. Proseedins of 1998 International Chemical Recovery Conference.

James Frederick. Black liquor properties. In Terry N. Adams, editor, *Kraft Recovery Boilers*. TAPPI Press, 1997.

James Frederick and Mikko Hupa. Black liquor droplet burning processes. In Terry N. Adams, editor, *Kraft Recovery Boilers*. TAPPI Press, 1997.

Thomas Grace and James Frederick. Char bed processes. In Terry N. Adams, editor, *Kraft Recovery Boilers*. TAPPI Press, 1997.

William C. Hinds. *Aerosol Technology Properties, Behavior, and measurement of airborne particles*. John Wiley & Sons, 2nd edition, 1999.

Willlliam C. Hinds. Physical and chemical processes in aerosol systems. In Pramod Kulkarni, Paul A. Baron, and Klaus Willeke, editors, *Aerosol Measurement - Principles, Techniques, and Applications*. John Wiley & Sons, 3rd edition, 2011.

Mikko Hupa. Recovery boiler chemistry. In Terry N. Adams, editor, *Kraft Recovery Boilers*. TAPPI Press, 1997.

J.R. Jensen, L.B. Nielsen, C. Schultz-Møller, S. Wendel, and H. Livbjerg. The nucleation of aerosols in flue gases with a high content of alkali- a laboratory study. *Aerosol Science and Technology*, (33:6):490–509, 2000.

J.K. Jokiniemi, J. Pyykönen, P. Mikkanen, and E.I. Kauppinen. Modeling fume formation and deposition in kraft recovery boilers. *TAPPI Journal*, (7):171–181, 1996.

J. Keskinen, K. Pietarinen, and M. Lehtimäki. Electrical low pressure impactor. *Journal of Aerosol Science*, 23:353–360, 1992.

K. N. Khan, M.M. Clay, and M. Silverman. Output characteristics of devilbiss no. 40 hand-held jet nebulizers. *European Respiratory Journal*, (3):1197–1201, 1990.

Saied Haghpanah Kochesfahani. *Particulate formation durin black liquor char bed burning*. PhD thesis, Toronto University, 1999.

Pramod Kulkarni, Paul A. Baron, and Klaus Willeke. Fundamentals of single particle transport. In Pramod Kulkarni, Paul A. Baron, and Klaus Willeke, editors, *Aerosol Measurement -Principles, Techniques, and Applications*. John Wiley & Sons, 3rd edition, 2011a.

Pramod Kulkarni, Paul A. Baron, and Klaus Willeke. Introduction to aerosol characterization. In Pramod Kulkarni, Paul A. Baron, and Klaus Willeke, editors, *Aerosol Measurement -Principles, Techniques, and Applications*. John Wiley & Sons, 3rd edition, 2011b.

Marko Marjamäki. *Electrical Low Pressure Impactor: Modifications and Particle Collection Characteristics*. PhD thesis, TUT Tampere, 2003.

Paterson McKeough. Understanding and predicting the release of sodium, potassium and chloride during black-liquor combustion in the recovery furnace. *TAPPI/PAPTAC International Chemical Recovery Conference*, 2010.

Paterson McKeough and Kauko Janka. Sulphur behaviour in the recovery boiler furnace: theory and measurements. *International Chemical Recovery Conference, Oral presentation*, 2001.

Paterson McKeough and E.K. Vakkilainen. Effects of black liquor composition and furnace conditions on recovery boiler fume chemistry. *International Chemical Recovery Conference, Oral presentation*, 1998.

P. Mikkanen, E.I. Kauppinen, J. Pyykönen, J.K. Jokiniemi, M. Aurela, E.K. Vakkilainen, and K. Janka. Alkali salt ash formation in four finnish industrial chemical recovery boilers. *Energy & Fuels*, (13):778–795, 1999.

P. Mikkanen, J.K. Jokiniemi, E.I. Kauppinen, and E.K. Vakkilainen. Coarse ash particle characteristics in a pulp and paper industry chemical recovery boiler. *Fuel*, (80):987–999, 2001.

Pirita Mikkanen. *Fly ash particle formation in kraft recovery boilers*. PhD thesis, Aerosol Technology group of VTT Chemical Technology, 2000.

Jukka Puhakka and Ossi Tolonen. On-line alkali measurement and control of the causticizing process. WWW, 2007. pointed at 7.6.2012.

John H. Seinfield and Spyros N. Pandis. *Atmospheric Chemistry and Physics from Air Pollution to Climate Change*. John Wiley & Sons, 2nd edition, 2006.

Sigma Aldrich. WWW Sigma Aldrich, 2011. pointed at 21.5.2012.

B.-J. Skrifvars, R. Backman, M. Hupa, K. Salmenoja, and E. Vakkilainen. Corrosion if superheater steel materials under alkali salt deposits part 1: The effect of salt deposits composition and temperature. *Corrosion Science*, (50):1274–1282, 2008.

TAPPI, 2001. Engineering/finishing & converting conference and trade fair, september 2001. TAPPI.

Alarick Tavares and Honghi Tran. Field studies on fume chemistry and deposition in kraft recovery boilers. *TAPPI Journal*, 80(12), 1997.

P. Tikka, editor. *Chemical Pulping Part 2, Recovery of Chemicals and Energy*. Paper Engineers' Association/Paperi ja Puu Oy, 2nd edition, 2008.

Honghi Tran and Esa K. Vakkilainen. The kraft chemical recovery process. *Proceedings of TAPPI Kraft Recovery Course, Section 1-1, TAPPI Press*, 2008.

Honhgi Tran. Recovery boiler corrosion. In Terry N. Adams, editor, *Kraft Recovery Boilers*. TAPPI Press, 1997a.

Honhgi Tran. Upper furnace deposition and plugging. In Terry N. Adams, editor, *Kraft Recovery Boilers*. TAPPI Press, 1997b.

Esa K. Vakkilainen. *Kraft recovery boilers- Principles and practise*. 2nd edition, 2005.

J. Yli-Ojanperä, J. Kannosto, M. Marjamäki, and J. Keskinen. Improving the nanoparticle resolution of the elpi. *Aerosol and Air Quality Research*, (10):360–366, 2010.

Appendix 1: Chemical Safety, reactant chemicals

Table 1: The table contains the chemicals fed to the test reactor. The list contains hazard and precautionary statements and incompatible chemicals for each chemical fed in the reaction chamber. (Sigma Aldrich, 2011)

Chemical	Hazard state-ments	Precautionary statements	Incompatible chemicals
Hydrochloric acid (HCl)	H314	P261	
	H335	P280	
		P305+P351+P338	
		P310	
Potassium hydroxide (KOH)	H302	P280	Water. Reacts violently with: metals, light metals. Contact with aluminum, tin and
	314	P305+P351+P338	zinc liberates hydrogen gas. Vigorous reaction with: alkali metals
		P310	
Sodium hydroxide (NaOH)	H314	P280	Strong oxidizing agents, strong acids, organic materials.
		P305+P351+P338	
		P310	

H280 Contains gas under pressure; may explode if heated.
H302 Harmful if swallowed.
H314 Causes severe skin burns and eye damage.
H315 Causes skin irritation.
H319 Causes serious eye irritation.
H335 May cause respiratory irritation.
P261 Avoid breathing gas.
P280 Wear protective gloves/protective clothing/eye protection/face protection.
P305+P351+P338 IF IN EYES: Rinse cautiously with water for several minutes. Remove contact lenses, if present and easy to do. Continue rinsing.
P310 Immediately call a POISON CENTER or doctor/physician.

Table 2: The table consists of the chemical compounds which can be assumed to form in the reaction chamber. The list contains hazard and precautionary statements and incompatible chemicals for each chemical possibly formed in the reaction chamber. (Sigma Aldrich, 2011)

Chemical	Hazard state-ments	Precautionary statements	Incompatible chemicals
Potassium chloride (KCl)	none		Strong acids, strong oxidizing agents.
Sodium chloride (NaCl)	none		Strong oxidizing agents.
Potassium carbonate (K_2CO_3)	H302	P261	Acids, strong oxidizing agents.
	H315	P305+P351+P338	
	H319		
	H335		
Sodium carbonate (Na_2CO_3)	H319	P305+P351+P338	Strong acids.
Potassium sulfate (K_2SO_4)	none		Strong oxidizing agents.
Sodium sulfate (Na_2SO_4)	none		Strong acids, Aluminum, Magnesium.

H302 Harmful if swallowed.
H315 Causes skin irritation.
H319 Causes serious eye irritation.
H335 May cause respiratory irritation.
P261 Avoid breathing gas.
P305+P351+P338 IF IN EYES: Rinse cautiously with water for several minutes. Remove contact lenses, if present and easy to do. Continue rinsing.

Appendix 3: Chemical Safety, gaseous chemicals

Table 3: List of gases used in these experiments. The list contains hazard and precautionary statements and incompatible chemicals or gases for each gas used in the reaction chamber.(Sigma Aldrich, 2011)

Gas	Hazard state-ments	Precautionary statements	Incompatible chemicals/gases
Carbon dioxide (CO_2)	H280	P410+P403	None.
Nitrogen (N_2)	H280	P410+P403	Strong oxidizing agents.
Sulphur dioxide (SO_2)	H280 H314 H331	P261 P280 P305+P351+P338 P310 P410+P403	Strong reducing agents, Zinc, strong oxidizing agents.

H280 Contains gas under pressure; may explode if heated.
H314 Causes severe skin burns and eye damage.
H331 Toxic if inhaled.
P261 Avoid breathing gas.
P280 Wear protective gloves/protective clothing/eye protection/face protection.
P305+P351+P338 IF IN EYES: Rinse cautiously with water for several minutes. Remove contact lenses, if present and easy to do. Continue rinsing.
P310 Immediately call a POISON CENTER or doctor/physician.
P410+P403 Protect from sunlight. Store in well-ventilated place.